DEVELOPMENT OF BIOFUNCTIONAL RUBY NANOPARTICLES FOR OPTICAL IMAGING OF OPIOID RECEPTORS

By

Rashmi Rajgopal Pillai

A THESIS SUBMITTED TO MACQUARIE UNIVERSITY
FOR THE DEGREE OF
MASTER OF RESEARCH
DEPARTMENT OF PHYSICS AND ASTRONOMY
APRIL 2017

MACQUARIE
University
SYDNEY·AUSTRALIA

Except where acknowledged in the customary manner, the work presented in this thesis is, to the best of my knowledge, original and has not been submitted elsewhere in whole or part for a degree in any university.

_____

Rashmi Rajgopal Pillai

Acknowledgements

I am deeply thankful to my families, both my parents and my in-laws, whose unconditional love and belief in my capabilities has kept me strong to pursue my higher studies. Special thanks to my loving husband, Sujish Kurup, for his endless love, understanding, and support through this challenging and rewarding journey. Thanks for standing by me and sharing with me the happiest moments in life. Special thanks to my grandma, her blessing and love has always been my greatest strength.

I am sincerely grateful to my supervisor Dr Varun Sreenivasan, for having me as his student, and providing me with the opportunity to strengthen my research skills in Macquarie University. I am very thankful for his enormous patience, and allowing me to have the freedom to carry out the research in my own way. He has always been very friendly, most positive, encouraging and supportive supervisor, without whom this project and thesis would not have happened.

I am deeply grateful to my supervisor A/Professor Andrei Zvyagin, for his constant support and valuable inputs. His helpful ideas and constructive comments have contributed a lot to improve the impact of my work and thesis.

I am also thankful to Prof Mark Connor for his welcoming attitude and helping us carry out cell labelling and imaging experiments in his facility.

I am also very thankful to my MRes advisor, Dr Joanne Dawson, for her support and inspiration throughout my MRes in Macquarie University. I appreciate her welcoming attitude and encouragement. I am also thankful to the admirable staff from the Department of Physics and Astronomy for their kind help throughout my MRes.

I acknowledge Macquarie University for awarding me the International Research Training Pathway Scholarship (iRTP), and research funding to pursue my MRes project. I am thankful to Centre for Nanoscale BioPhotonics (CNBP) for providing me with the research infrastructure and smooth work environment.

I would also like to thank all my wonderful friends, Martin, Alex, Sandhya, Piotr, Zosia, Denitza, Olivia, Annie, Wei, Lianmei, Shivani and Hindol for lending me their ears, offering me their advice, supporting and cheering me up throughout this last ten months. I also appreciate and thank my friends from chemistry and biology departments. The good times we

had, coffee/ lunch breaks, games nights, numerous outings are all greatly appreciated. Thanks, guys for making my stay in Australia memorable and enjoyable.

Conference Posters and Presentations

1. Rashmi Pillai, Varun Sreenivasan, Mark Connor, Andrei Zvyagin, "Towards live-imaging of opioid receptors with nanoruby"; 6th Annual Macquarie Biofocus Research Conference, December **2016.**
2. Rashmi Pillai, Varun Sreenivasan, Mark Connor, Andrei Zvyagin, "Development of biofunctional ruby nanoparticles for optical imaging of opioid receptors"; the 8th International NanoMedicine Conference, July **2017.**

Abstract

There is an increasing demand for high performance photoluminescent nanoparticles in the life sciences, where the targeted labelling and optical imaging of biomolecules are needed. Photostability, low environmental sensitivity and narrow spectra make nanoparticles superior over existing molecular fluorophores. Ruby nanocrystals, termed nanorubies, represent an excellent example, especially their long photoluminescence lifetime allowing dramatic improvement of the optical contrast. However, premature surface functionalisation procedures have hindered the widespread use of nanorubies.

To address this challenge, the first aim was to develop facile and reproducible protocols to functionalise nanoruby with biomolecules, specifically, NeutrAvidin. The second aim was to demonstrate the use of developed biofunctional nanorubies to label opioid receptors in live and fixed cells, followed by high-sensitivity optical imaging.

Silica nanoparticles formed a test-bed to develop conjugation methods based on amide and click chemistries. Biotin-binding assays and receptor labelling studies showed that click chemistry was most specific, efficient, reproducible and controllable. Amide-based chemistries, in comparison, resulted in non-specific binding and low-contrast imaging. The developed click chemistry protocol, when extended to silica-coated nanorubies, allowed specific labelling and high-sensitivity imaging of opioid receptors.

This study enables the wide use of nanoruby for ultrasensitive and real-time imaging of a broad class of receptor-ligand systems.

Contents

List of Figures

Abbreviations

PL	Photoluminescent
NPs	Nanoparticles
SiNR	Silica-coated ruby nanoparticles
SiNR-NA	Silica-coated ruby nanoparticles-NeutrAvidin
SNP	Silica nanoparticles
SNP-NA	Silica nanoparticles-NeutrAvidin
QD	Quantum dots
MORs	μ-opioid receptors
GPCR	G-protein coupled receptor
NA	NeutrAvidin
EA	Ethanolamine
BSA	Bovine Serum Albumin
DBCO	Dibenzocyclooctyne
PEG	poly- (ethylene glycol)
EDC	1-ethyl-3-(3-dimethylaminopropyl) carbodiimide
NHS	N-hydroxysuccinimide
DLS	Dynamic Light Scattering
FTIR	Fourier Transform Infrared spectroscopy
HA-hMOR	HA-epitope tagged human mu-opioid receptors
FLAG-mMOR	N-terminally FLAG-epitope tagged mouse mu-opioid receptors
DMEM	Dulbecco's Modified Eagle Medium
FBS	Fetal Bovine Serum

Chapter 1. Introduction

Observation of molecular processes and their interactions in living cells is fundamental to obtain a quantitative understanding of larger biological functions. Over the past decade, most of the scientific and technological efforts have been focussed on untangling the complexity of these interactions, which often spans large time- and length-scales[1]. Advances in the areas of molecular detection[2], microscopy[3] and labelling techniques[4] has accelerated our pursuit towards this goal.

More recently, nanotechnology has been playing a progressively significant role to solve challenges at small-length scales. Nanotechnology refers to the control and manipulation of structures at the nanoscale, where unique properties of the material may be witnessed[5]. The significance of nanotechnology extends to several sectors, including healthcare[6], food[7], research, defence and environment[8]. A class of nanomaterials, called photoluminescent nanoparticles, is particularly suited for applications in the life sciences and they are of interest to this thesis.

Photoluminescent nanoparticles are suitable as probes for biomolecular labelling and imaging applications, where they allow detection and tracking of molecular processes and interactions[9]. As photoluminescent probes, most nanoparticles overcome many limitations of conventional molecular fluorophores such as photobleaching, blinking, susceptibility to the environment, spectral overlap etc.[1]. These properties have resulted in major advances in molecular and cell biology, including investigations of cellular morphology and various processes in cells and tissues in their full biological context[9]. Besides, nanoparticle surfaces can be conjugated with biomolecules of interest, which can target and interact specifically within a biological system[10]. Nanoparticles are also extensively used and developed as delivery vehicles for drugs[11, 12] or genes[11] to targeted locations, which is of clinical relevance.

The goal of this thesis is to engineer the surface of a specific type of photoluminescent nanoparticle, called nanoruby, and to apply it to label G-protein coupled receptors on living cells to allow imaging at the single-particle sensitivity.

1.1 Motivation and research objectives

μ-opioid receptors (MORs) are targets for the most effective pain-relieving drugs, such as morphine[13]. MORs belong to the G-protein coupled receptor (GPCR) family, and like most other GPCRs, understanding the expression, structure, function, downstream

signalling and regulation of MOR is of major scientific interest[14]. Since MOR are of clinical relevance, advances in this area is crucial for developing better drugs for analgesia, with reduced desensitization and side-effects[13]. Unravelling the fine details of the location and molecular mechanisms of drug-action is currently an area of major scientific activity.

Photoluminescent (PL) nanoparticles (NPs) are suitable to address these questions. In particular, nanoruby – one of the newly discovered and promising PL nanomaterial developed within our group[15] – has shown considerable promise for molecular labelling, imaging and tracking of single molecules. This is because the photoluminescence of nanoruby is extremely photostable (no photobleaching or blinking)[15], and its property of long photoluminescence lifetime (discussed in detail in next Chapter) allows imaging at ultra-high sensitivity[16]. However, the application of nanoruby towards labelling and imaging of cell surface receptors, such as the MOR, has been challenging.

For example, in an earlier study from our group [unpublished results], silica-coated nanorubies (SiNR) were surface functionalised with biotin label-MORs using a three-step streptavidin sandwich method schematised in Figure 1.1(a). Briefly, a biotinylated antibody targeted an extracellular epitope of the MOR. A tetravalent streptavidin molecule is added to bind to the biotin tag of the antibody. The biotinylated SiNR then binds to the immobilised streptavidin, resulting in nanoruby indirectly binding to MOR. This resulted in specific and reproducible labelling of MORs present on the cell membrane, but only in fixed cells [Figure 1.1(e)]. This method was inefficient in labelling membrane-bound receptors in live cells [Figure1.1(i)], despite using identical labelling conditions, including temperature and reagents.

The inefficiency of three-step labelling method was investigated further and could be due to one or more of the following factors. Firstly, biotinylated commercial fluorescent silica nanoparticles (SNP-PEG(B)) were used to test issues with functionalisation of SiNR (Figure S1a). Secondly, a protease inhibitor cocktail was used to test potential cleavage of streptavidin bound to live cells, but the labelling remained unchanged (Figure S1b). Thirdly, we used dye-labelled biotin to test whether the mobile nature of cell membrane could result in re-organisation of the membrane proteins. However, dye-labelled biotin bound equally well in fixed and live cells (Figure S1c). Our next experiment pointed that cellular mechanism that occur after streptavidin labelling prevents access of nanometre sized particles to membrane proteins. The receptors once bound with biotinylated antibody

or streptavidin may lead to clustering or formation of membrane invaginations which may hamper the labelling of live cells by preventing access to 100-nm particles. It was hypothesized that reducing the number of labelling steps from three to two, by using streptavidin-conjugated nanorubies, will improve the labelling performance.

Thus, a focus of this thesis was to develop strategies to functionalise the surface of silica-coated nanoruby and conjugate a functional and cost-effective analogue of streptavidin, called NeutrAvidin. The end goal was to demonstrate that such a nanoruby-NeutrAvidin conjugate can be used to label MORs in live cells, for single-particle sensitive photoluminescence imaging. The use of commercially available silica nanoparticles as a model for silica-coated nanoruby facilitated the success of the nanoruby bioconjugation and application. The protocols for functionalising nanoparticle surface and conjugating NeutrAvidin were first developed using silica nanoparticles, and then extended to silica-coated nanoruby.

The main objectives of this research work were the following:

1. To test three methods to functionalise model silica nanoparticles (SNP);
2. To test three methods to covalently conjugate the functionalised SNP with NeutrAvidin;
3. To extend the best of the three methods to conjugate silica-coated nanoruby with NeutrAvidin;
4. To label and image MORs using the conjugates in live and fixed cells.

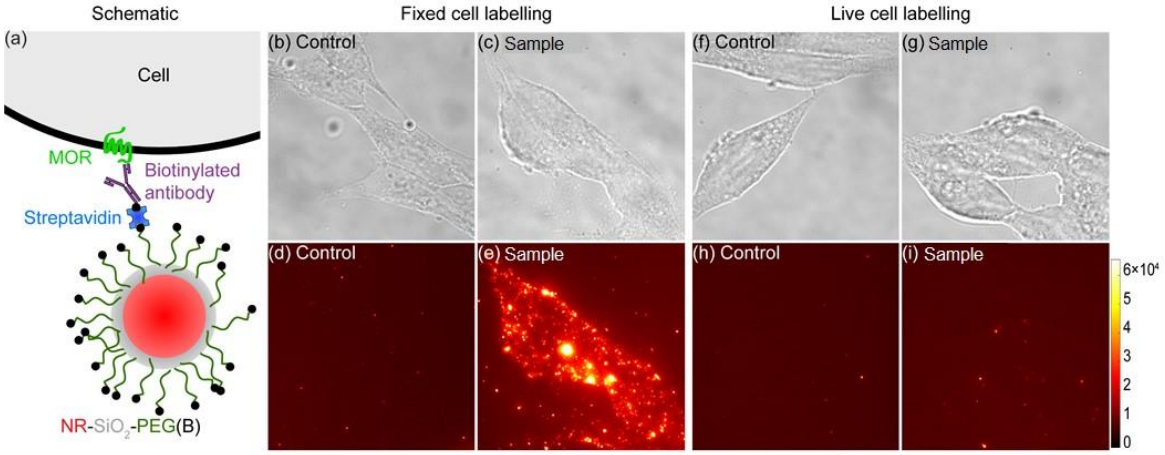

Figure 1.1. (a) Schematic representation of the three-step streptavidin-sandwich based labelling of MOR using silica-coated and biotinylated nanoruby (NR-SiO_2-PEG(B)). Labelling of MORs in (b-e) fixed and (f-i) live cells. Control was labelling of a variant of

MOR that is not recognised by the antibody. Top and bottom rows show bright field transmission images of cells and nanoruby photoluminescence (false color, colorbar on bottom right), respectively. The dimensions of the images are 130 µm x 130 µm.

1.3 Research framework

This nine-month Master of Research project commenced in July 2016 at the Department of Physics and Astronomy at Macquarie University in Sydney, Australia. As per the guidelines set by the Department, the main text of this thesis must not exceed 50 pages.

1.4 Thesis Outline

This thesis contains **6 chapters**:

- Introductory chapter
  - — Chapter 2 covers concepts and recent advances in nanotechnology, surface chemistry.
- Experimental methodology
  - — Chapter 3 documents the characterisation techniques and experimental procedures used throughout this project.
- Experimental results and discussions
  - — Chapter 4 contains results obtained during development, characterisation, and optimisation of functionalisation and conjugation strategies for the model SNP. The developed SNP conjugate was used to label and image MOR.
  - — Chapter 5 contains results obtained upon extending the functionalisation and conjugation strategy developed in Chapter 4 to silica-coated nanoruby. The developed strategy nanoruby conjugate enabled specific labelling and sensitive imaging of MOR in live and fixed cells.
- Conclusion and future perspective
  - — Conclusions from this work are presented in Chapter 6, along with a view on its future perspectives.

References

1. Zvyagin, A.V., et al., *Luminescent nanomaterials for molecular-specific cellular imaging*, in *Handbook of nano-optics and nanophotonics*. 2013, Springer. p. 563-596.

2. Giepmans, B.N., et al., *The fluorescent toolbox for assessing protein location and function.* science, 2006. **312**(5771): p. 217-224.

3. Diaspro, A., *Confocal and two-photon microscopy: foundations, applications and advances.* Confocal and Two-Photon Microscopy: Foundations, Applications and Advances, by Alberto Diaspro (Editor), pp. 576. ISBN 0-471-40920-0. Wiley-VCH, November 2001., 2001: p. 576.

4. Wang, F., et al., *Luminescent nanomaterials for biological labelling.* Nanotechnology, 2005. **17**(1): p. R1.

5. Pradeep, T., *A textbook of nanoscience and nanotechnology*. 2012: Tata McGraw-Hill Education.

6. Fakruddin, M., Z. Hossain, and H. Afroz, *Prospects and applications of nanobiotechnology: a medical perspective.* Journal of nanobiotechnology, 2012. **10**(1): p. 31.

7. Sozer, N. and J.L. Kokini, *Nanotechnology and its applications in the food sector.* Trends in biotechnology, 2009. **27**(2): p. 82-89.

8. Bhushan, B., *Springer handbook of nanotechnology*. 2010: Springer Science & Business Media.

9. Sreenivasan, V.K., A.V. Zvyagin, and E.M. Goldys, *Luminescent nanoparticles and their applications in the life sciences.* Journal of Physics: Condensed Matter, 2013. **25**(19): p. 194101.

10. Conde, J., et al., *Revisiting 30 years of biofunctionalization and surface chemistry of inorganic nanoparticles for nanomedicine.* Frontiers in chemistry, 2014. **2**: p. 48.

11. Mahon, E., et al., *Designing the nanoparticle–biomolecule interface for "targeting and therapeutic delivery".* Journal of Controlled Release, 2012. **161**(2): p. 164-174.

12. Veronese, F. and M. Morpurgo, *Bioconjugation in pharmaceutical chemistry.* Il Farmaco, 1999. **54**(8): p. 497-516.

13. Al-Hasani, R. and M.R. Bruchas, *Molecular mechanisms of opioid receptor-dependent signaling and behavior.* The Journal of the American Society of Anesthesiologists, 2011. **115**(6): p. 1363-1381.

14. Galés, C., et al., *Real-time monitoring of receptor and G-protein interactions in living cells.* Nature methods, 2005. **2**(3): p. 177-184.

15. Edmonds, A.M., et al., *Nano-Ruby: A Promising Fluorescent Probe for Background-Free Cellular Imaging.* Particle & Particle Systems Characterization, 2013. **30**(6): p. 506-513.

16. Razali, W.A., et al., *Wide-field time-gated photoluminescence microscopy for fast ultrahigh-sensitivity imaging of photoluminescent probes.* Journal of biophotonics, 2016.

Chapter 2. Photoluminescent probes- functionalisation and applications in molecular imaging

This introductory chapter contains basic information and recent scientific progress relevant to this thesis, and is divided into two parts. The first part contains fundamentals of photoluminescence and fluorescence microscopy. It also includes brief discussions of the conventional photoluminescent probes and their shortcomings, followed by novel photoluminescent probes including nanorubies. The second part contains concepts of surface chemistry, including functionalisation and approaches to conjugate nanoparticles with biomolecules.

Contents

2.1 Fundamentals of photoluminescence

Some materials emit light by a process called luminescence, following an excitation process. Photoluminescence is one type of the luminescence, where light emission follows the absorption of light energy[1]. In this process, a molecule absorbs a photon whose energy (and hence wavelength) meets the molecule resonance condition, makes a transition to the excited energy state, and emits a photon, when making a transition to the ground energy state[2]. Often, a process of the photon excitation and emission entails a photon energy penalty, which is dissipated in the form of vibrational relaxations, so that the emitted photon is generally "red-wavelength-shifted" – the effect is known as Stoke's shift[1]. The process of photoluminescence is also characterised by a photoluminescence lifetime.

2.1.1 Photoluminescence lifetime

Photoluminescence lifetime (τ) is the mean time taken for molecules in the excited states to decay to the ground state. More precisely, it is defined as the time taken for the photoluminescence intensity to reduce to $1/e$ of its initial value, since the intensity decay generally follows an exponential function. For the purposes of this thesis, it is important to recognise that there are two regimes of photoluminescence that differ by their photoluminescence lifetime - fluorescence or phosphorescence. Most photoluminescent materials (organic and inorganic) are characterised by lifetimes, ranging from tens of picoseconds to tens of nanoseconds. Some molecules and new generation nanoparticles are characterised by the lifetimes ranging from microseconds to milliseconds. Photoluminescence occurring within τ ranging from picoseconds to nanoseconds and from microseconds to seconds are called fluorescence and phosphorescence, respectively. The molecular transitions between energy levels that give rise to the two phenomena are depicted in Figure 2.1. Since both fluorescent and phosphorescent materials are used in this work, the term photoluminescence is used in general, instead of fluorescence or phosphorescence. The use of phosphorescent materials is advantageous because their emission can be discriminated from that of fluorescent materials, which are abundant in biological systems[3]. This aspect will be discussed in detail later in this chapter.

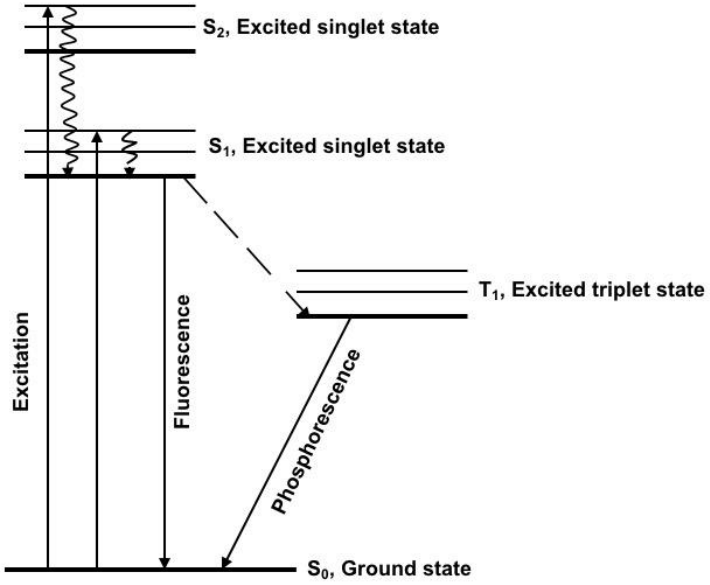

Figure 2.1 Jablonski energy diagram demonstrating the phenomena of fluorescence and phosphorescence[2, 3].

2.1.2 Photoluminescence imaging

Photoluminescence microscopy is a very popular method for measuring structural, organizational, and dynamic properties of biological and biomolecular systems[4], and is of relevance to this thesis. The technique relies on the contrast provided by photoluminescent molecules (either introduced or endogenous) in a sample. Photoluminescent molecules or nanoparticles introduced into a biological sample to increase the imaging contrast are generally termed photoluminescent (PL) probes[5] (discussed in section 2.1.3).

The importance of PL microscopy has increased significantly in the last two decades, primarily due to the development of sophisticated photoluminescent molecular probes. A conventional photoluminescence microscope can allow visualization of single molecules or nanoparticles separated by several hundred nanometres, as determined by the Rayleigh criterion, in pristine imaging conditions. However, the sensitivity and resolution of imaging is ever increasing. With the development of time-gated fluorescence microscopy[6], multi-photon fluorescence microscopy[7], and many recently developed super-resolution microscopy techniques[8], it is now possible to image single molecules or nanoparticles in highly scattering and even fluorescent-probe stained samples, and image with 20-30 nm resolution[4]. Despite these advancements, uptake of PL microscopy in Life Sciences is slow due to the performance limitation of the most existing PL probes.

2.1.3 Photoluminescent probes – current limitations and emergence of new probes

Some of the commonly used probes for PL microscopy include organic molecules such as Alexa Fluor, Cyanine 5, Rhodamine, Fluorescein and fluorescent proteins (e.g., green fluorescent protein)[5]. However, these probes become non-fluorescent after about a million excitation-emission cycles, because they undergo irreversible "photobleaching"[5]. This practically limits the duration and reliability of imaging, and therefore tracking of single molecular processes. Some PL probes are also toxic, while others do not tolerate changes in chemical and biological environments such as pH or hydrophobicity. Although the design of improved quality organic fluorophores is in continuous progress, there is a strong demand for alternative solutions. In the past decade or so, developments in nanotechnology has resulted in photoluminescent (PL) nanoparticles (NPs). They address some of the limitations of conventionally used PL probes.

Some of the well-established nanoparticle PL probes include quantum dots[9], fluorescent nanodiamonds and upconversion NPs[10]. Some relevant properties of these probes are discussed in the Table 2.1. Nanodiamonds and upconversion NPs are photostable, producing unfading emission. They exhibit limited or no cytotoxicity[10]. Lanthanide–based NPs also offer high-contrast detection by means of the time-gated imaging[11, 12]. However, these NP-based molecular probes are still not ideal. For example, upconversion NPs require high excitation intensity due to their nonlinear excitation characteristics and are susceptible to emission quenching; nanodiamonds exhibit poor photoluminescence intensity combined with low contrast in autofluorescent samples; cytotoxicity of several types of NPs, including carbon nanotubes and semiconductor quantum dots are still under debate. And quantum dots exhibit photoluminescence blinking, where they transiently appear bright and dark under a microscope. Therefore, there is continuing interest in developing alternative PL NPs with improved properties.

	Organic Dye	QDs	UCNPs	FNDs	Nanorubies
Excitation	UV/Visible	UV/Visible	Near IR	Visible	Visible
Emission (nm)	405-805	400-1400	300-900	575, 637	692,694
Lifetime	< 10ns	10 – 20ns	100 – 10ms	10 – 20ns	3ms
Non-photobleaching	x	√	√	√	√
Non-blinking	x	x	√	√	√
Non-toxicity	x	x	√	√	√

Table 2.1 Comparison of properties of various photoluminescent probes[5, 10, 11]. Abbreviations: QD (quantum dot), UCNP (upconversion nanoparticle), FND (fluorescent nanodiamonds).

2.2 Nanoruby

Nanoruby (NR) is newly discovered PL nanomaterial that exhibits photoluminescence and physical properties offering advantages with respect to PL microscopy (compare in Table 2.1). NRs are nanometre-sized crystals of a gemstone ruby whose red-colouration results from chromium Cr^{3+} ion substitutions in the alumina crystal (α-phase, Al_2O_3)[13]. These colour centres are also the origin of the photoluminescence of NR. Light energy absorbed in the blue-green region by NR is re-emitted as a sharp spectral peak at 692 nm.

2.2.1 Characteristic features of nanoruby

NR exhibit several unique physicochemical and photophysical properties, including virtually unlimited photostability and long photoluminescence lifetime (≈ 3.7ms)[14], superior brightness, a narrow photoluminescence emission band at 692 nm, high quantum yield reaching 90% in bulk and biocompatibility[13]. The long PL lifetime of NR has been reported to be advantageous for imaging samples with high autofluorescence background[15]. This is possible because time-gated imaging allows the temporal discrimination of short (ns) lifetime autofluorescence from endogenous fluorescent molecules within biological samples and long PL lifetime of NR. Time-gated imaging makes use of PL millisecond scale emission and is realised by turning on a photoreceiver, following a short time delay after the excitation light pulse terminates. The ability to discriminate probes with long PL lifetime from more rapidly decaying optical background

gives time-gated microscopy an edge over other methods, and has demonstrated orders of magnitude increase in detection sensitivity of NR[15]. These properties combined with low production cost[unpublished] makes NR an attractive PL probe. As described in Chapter 1, the use of NR for biomolecular labelling and imaging application is currently challenged by the ability to functionalise the nanoruby surface.

2.3 Functionalisation of PL NPs

2.3.1 Introduction and importance of functionalisation

In recent years, considerable efforts have been devoted to functionalising PL NPs for biomedical imaging and sensing applications. Functionalisation involves surface modification strategies, such as introduction of polymer or silica or small molecules to introduce intermediate reactive chemical functional groups (Figure 2.2). These groups provide chemical anchors to immobilize biomolecules of interest by the second process called bioconjugation[16-18]. The functionalisation is sometimes also used to enhance the water-dispersibility and/or biocompatibility of nanoparticles.

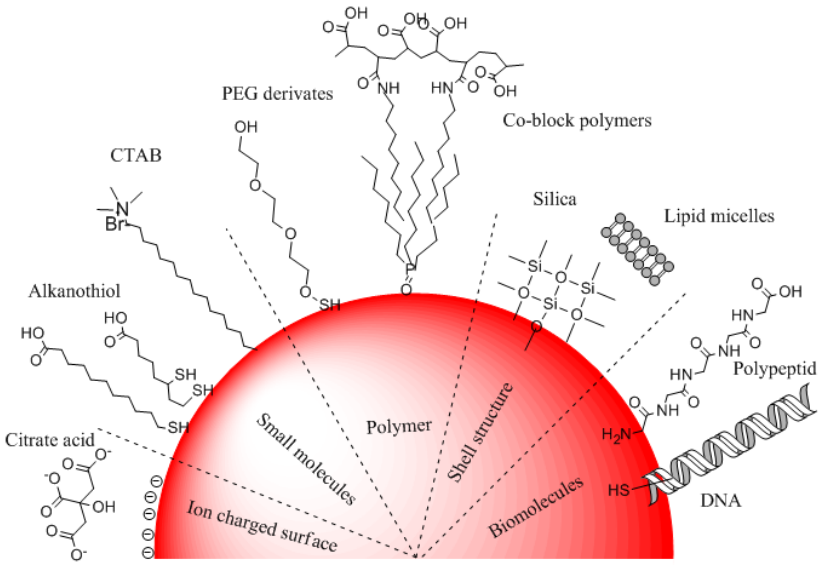

Figure 2.2 Common strategies used for surface functionalisation of NPs[16, 17].

2.3.2 Considerations and requirements of NP functionalisation and conjugation

A number of factors need to be considered when designing and carrying out nanoparticle functionalisation and conjugation. These include the NP surface chemistry, the functional groups to be introduced, choice of a linker, an efficient conjugation reaction between the functional group and biomolecule to be conjugated, and finally the conditions (pH, temperature, ionic strength, solvent choice) to ensure maximum reaction

efficiency[17]. The final application of the nanoparticle conjugate may also be important when evaluating the conjugation strategy[16]. The ideal outcomes of a conjugation process must be the retention of biological function of the conjugated biomolecules, unaffected PL signal of the nanoparticle and colloidal stability of the conjugate. Some of the frequently used functionalisation strategies that will be used in this work are discussed below.

2.3.3 Functionalisation strategies

2.3.3.1 Polymer coatings- poly (ethylene glycol) (PEG)

In recent years, polymer coatings[17] have been extensively investigated to enhance the biocompatibility of nanoparticle system. This can be attributed to their unique physical or chemical properties which increases repulsive forces to balance the Van der Waals attractive forces acting on the NPs (steric stabilisation)[19]. Most commonly used polymer to modify nanoparticle surface is called poly(ethylene glycol) (PEG)[20], which is a coiled polymer comprising repeating ethylene glycol units, available in a wide range of chain lengths and a number of terminal reactive functional groups. It is an inert and biocompatible polymer due to its simple structure and chemical stability. It is well soluble in water and serum, and in several organic polar and non-polar solvents. PEG functionalised NPs generally show reduced aggregation in biological media owing to the passivated surfaces and lack of protein corona resulting in so-called `stealth' behaviour[17, 19, 21]. These features of PEG functionalised NPs are exploited in several applications such as pharmaceutical formulations[22-24] and medical imaging[16].

2.3.3.2 Silica

Another strategy for functionalisation of NPs is by modification with a silica shell. This is most widely used for NPs that either has problems with agglomerations\, or are difficult to functionalise. Silica coating offers the following advantages: (a) it minimises the interparticle interactions and prevents agglomeration, (b) imparts good biocompatibility, hydrophilicity and stability, and (c) it introduces hydroxyl groups which can be used to covalently introduce reactive moieties (including amino, carboxyl) using silane based chemistry[25]. This strategy has been widely used to modify nanoparticles of various materials, in particular metal oxide nanoparticles (e.g. nanoalumina[26]), noble metals (Au[27]; Ag[28]), fluorescent quantum dots (CdSe/ZnS[29-31]), and magnetic nanoparticles (e.g. Fe_2O_3[32]). More detailed descriptions of the silica-coating applications can be found in the bespoke citations. However, there are instances where organic phase

synthesis of silica-coated nanoparticles has a major disadvantage that additional steps are needed after synthesis to stabilise the particles in aqueous medium which can lead to irreversible aggregation of the particles or they show buffer instability by agglomerating especially in phosphate-buffered solutions[33].

Thus, these functionalisation strategies modify the nanoparticle surface and introduce functional chemical groups, which act as anchor points for immobilising biomolecules by the process of conjugation. Some of the reported conjugation strategies are discussed in the next section.

2.4 Conjugation strategies

Several strategies have been documented for the conjugation of PL NPs with biomolecules and they can be broadly categorised into (i) non-covalent interactions, such as physical adsorption, electrostatic, hydrophobic/hydrophilic interactions and (ii) covalent chemistries, such as carbodiimide chemistry, click chemistry. Figure 2.3 lists a broad spectrum of conjugation strategies evaluated in the literature[34, 35].

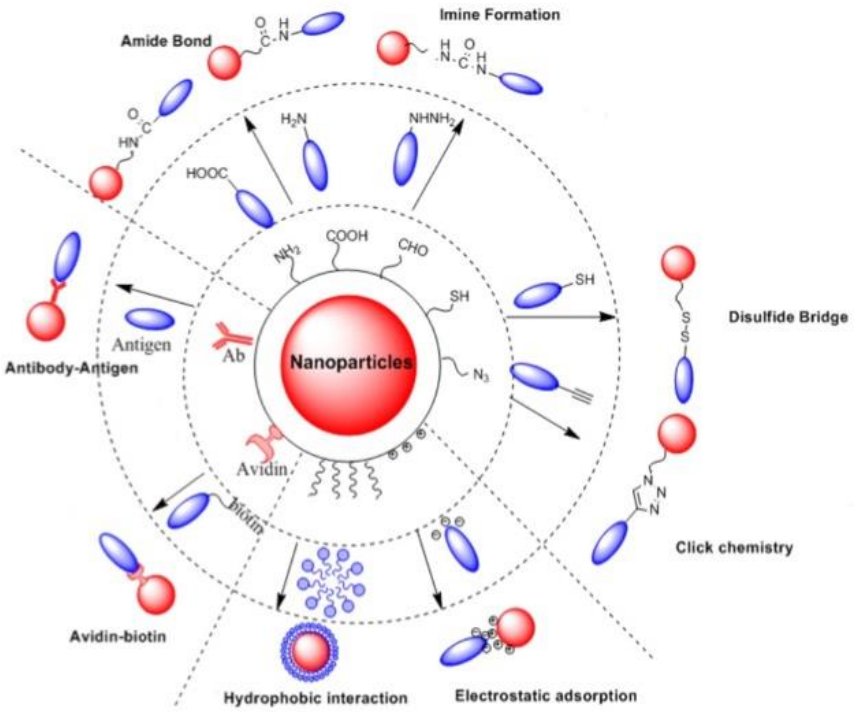

Figure 2.3 Common conjugation methods used for attaching biomolecules with NP after functionalisation[34, 35].

2.4.1 Noncovalent interactions

Noncovalent interactions, including electrostatic and hydrophilic/hydrophobic

interactions, between biomolecules and NPs have been frequently used to immobilise NPs with small organic substances and large protein/ enzyme molecules[36]. Electrostatic ionic coupling has been traditionally used to adsorb biomolecules to NPs such as proteins[37, 38]; DNA[39]; and siRNA[40]. Similarly, hydrophobic molecules, such as fluorophores[41] or lipid drugs[42] are coupled to hydrophilic NPs using this method. Despite the ease of this conjugation method, the generated conjugates are often unstable and the reactions are poorly reproducible. This conjugation technique may also result in the loss of biological activity of the adsorbed biomolecules[43, 44].

2.4.2 Covalent conjugation

Covalent conjugation is an attractive strategy as it results in a stable and irreversible link, unlike those formed by hydrophobic and electrostatic non-covalent interactions[34, 35]. It is based on attachment of biomolecules to NP surface by the formation of covalent inter-atomic bonds[45]. Development and testing of different covalent conjugation chemistries for PL NPs form an integral part of this thesis work. The reactive chemical groups (such as carboxyl, NHS ester and azide) introduced on the PL NPs surface by functionalisation step are used to form covalent bonds with the amine terminals of a protein of interest, as described below.

2.4.2.1 Carbodiimide chemistry

The most standard and widely used covalent conjugation method is carbodiimide chemistry[34]. The carbodiimide chemistry can be executed in two ways: amine containing NPs can couple to a carboxyl group containing biomolecule, or vice-versa. The chemistry requires a catalyst known as 1-ethyl-3-(3-dimethylaminopropyl) carbodiimide (EDC). This carbodiimide cross linker activates carboxyl groups and forms amine reactive O-acylisourea intermediate that spontaneously reacts with primary amines to form an amide-bond[46]. N-hydroxysuccinimide (NHS) is often used in addition to EDC to increase the reaction yield, as it stabilises the amine-reactive intermediate by converting it to an amine reactive NHS ester[47]. Advantage of this chemistry is fast reactivity, water solubility, and easy removal of excess reagents[35]. This approach has been used in the attachment of a variety of biomolecules including DNA, proteins, peptides, antibodies to NPs[16]. For instance, using the EDC chemistry, Weissleder et al. created a library of magnetic NPs decorated with different synthetic small molecules for developing magneto-fluorescent reporters[48]. Lee et.al[49] developed a route using this chemistry for conjugating the γ-

Fe_2O_3 NPs with single strand oligonucleotides. This strategy is also extended for conjugation of the other nanostructured materials, such as gold NPs and carbon nanotubes[50].

However, this method has some drawbacks, as the reactive ester intermediate readily hydrolyses in aqueous solutions, resulting in a loss of the conjugation efficiency. The reaction is also dependent on pH, as EDC crosslinking is efficient in the acidic pH range (4.5 - 6.5), whereas NHS ester reaction are more efficient at pH 7-8.5[45]. These factors reduce the reproducibility of the conjugation, affecting efficiency and stability[34]. Some relief from these issues is available to researcher's due to commercial availability of preformed NHS-ester terminated reagents, as discussed in the following section.

2.4.2.2 NHS ester chemistry

NHS esters are reactive groups formed by the activation of carboxyl molecules, and they spontaneously react with primary amines of biomolecules to form an amide bond[46]. Linkers that are terminated with NHS esters are available commercially. The reaction is theoretically simple, as it does not require catalysts. However, in practise the dependence of the reaction on pH can result in poor conjugation efficiency and reproducibility. At low pH, the amine group of the protein biomolecule to be conjugated exists in its protonated form, thus preventing reaction. Meanwhile at higher-than-optimal pH, the NHS ester hydrolyses very quickly (NHS esters have a half-life of 4-5 hours at pH 7, 2 hours at pH 8 and only 10 minutes at pH 8.6-9.0)[35], resulting in reduced conjugation yield. In literature, this approach has been widely used to modify proteins and peptides[51], however, less often to conjugate NP surface with biomolecules (some e.g., are DNA and aptamers[52], peptides, and fluorescent molecules). Advances in different methods for specific and efficient conjugation of nanoparticles with biomolecules have given rise to a relatively newer approach, which is discussed next.

2.4.2.3 Click chemistry

Click reactions are spontaneous chemical reactions that occur between two specific molecular groups, which are otherwise non-reactive[53]. Due to the specificity and efficiency, they have been applied extensively in polymer chemistry and materials engineering[54, 55]. Azide and alkyne groups form one such "click pair" that form stable covalent bonds based on a cyclo-addition reaction[56, 57]. Due to their inertness is biological media, and high efficiency in aqueous solution, the azide-alkyne cycloaddition

reaction has been extensively used for nanoparticle conjugation. The process is carried out by first functionalising a nanoparticle and a protein of interest by azide or alkyne. Addition of the azide-functionalised nanoparticle and alkyne-functionalised protein in aqueous solution results in a stable conjugate[57]. Among the improvements made to this chemistry, the following are notable. The earlier versions required the use of copper as a catalyst. However, copper is cytotoxic and it needs to be maintained in the correct oxidative state for the efficient reaction. Recently, several copper free click ligands have been developed, including cyclooctynes[58]. They harbour a high-strain ring structure that react readily with azide, avoiding the need for a catalyst[58].

Compared to the other covalent chemistries, click chemistry offers several advantages. Firstly, azide and alkyne reactive groups are highly specific to one another, and unreactive with the most functional groups, ensuring specific conjugation at a desired location. Secondly, the formed bonds are stable. Thirdly, the reaction is fast and efficient, requiring mild reaction conditions (aqueous environment, relatively neutral pH), and create water-soluble and biocompatible conjugates. Click chemistry based reactions has been successfully employed to conjugate nanoparticles with biomolecules such as AuNPs to proteins[59], enzymes[60], fluorophores[61] and polymers[62].

2.5 Affinity interaction

The specificity and efficiency of biomolecule conjugated PL NPs for molecular imaging can be further improved by affinity interactions. This method relies on strong and specific complementary recognition interactions between an affinity molecular pair such as antigen-antibody[63], streptavidin-biotin[64-66], aptamer-protein[67], complementary nucleotide sequences[46], etc.

2.5.1 Streptavidin-Biotin molecular pair

Over the years, streptavidin-biotin interaction has been applied in numerous laboratory methods, especially in the areas of immunolabelling and molecular biology. Streptavidin derives its name from the bacterial source of the protein, *Streptomyces avidinii*, and from egg-white avidin. Both avidin and streptavidin exhibit extraordinary ligand binding affinity for biotin, a vitamin H molecule ($K_d \approx 10^{-15}$ M)[68, 69]. They are eminent example of molecules that constitute an affinity molecular pair in nature.

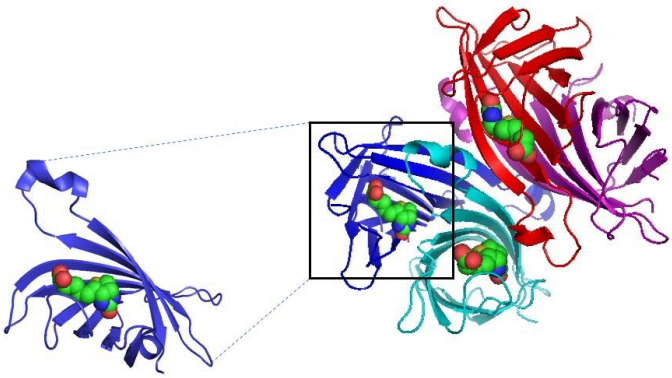

Figure 2.4 Tetrameric structure of Streptavidin (ribbon diagram) bound to biotin (ball model). Inset is the monomeric streptavidin with bound biotin[70].

Streptavidin has a tetrameric structure and each subunit has a single binding site for biotin. This multivalent structure increases their functionalisation efficiency while still retaining its biological activity. They have no carbohydrates and has an acidic near-neutral isoelectric point (pI ≈ 6.8-7.5), which results in a lower degree of nonspecific binding. These proteins also exhibit resistance to extreme temperatures (i.e., midpoint temperature of denaturation, Tm of 112ºC for biotin-streptavidin), pH conditions, denaturing agents, and enzymatic degradation[71]. Also, biotinylated molecules such as biotinylated antibodies, proteins, enzymes, etc., are easily available commercially. However, streptavidin shows some drawbacks which includes first, it is costlier to produce; and second, the RYG sequence (structurally mimics the ubiquitous cell adhesive RGD sequence) creates specificity issues in certain applications[68, 72].

2.5.2 Analogue of Streptavidin- NeutrAvidin

In recent years, a much more ideal and cost-effective avidin derivative has been synthesised. It is known as deglycosylated avidin or NeutrAvidin (NA)[73, 74]. NA (60,000 Da) has a reduced mass as compared to avidin (67,000 Da) but retains its high biotin-binding affinity. Deglycosylation of avidin reduces lectin binding to undetectable levels and lowers the isoelectric point (pI=6.3). It also lacks the “RYD” sequence, thus effectively eliminating the major causes of nonspecific binding. Because lysine residues remain available, NA can be conjugated as easily as streptavidin[17]. The main method of bioconjugation using NA-biotin chemistry comprises the functionalization of NPs with NA, for later incubation with a biotinylated molecule. This strategy has been widely used to immobilise biotinylated proteins[75, 76], DNA[65, 66], enzyme[64] on different class

of NPs. The remarkable characteristics of this affinity molecular-pair makes them very useful in molecular labelling and imaging applications.

2.6 Summary

The power of PL microscopy has increased significantly in the last two decades, primarily due to the development of sophisticated photoluminescent molecular probes, which enables highly specific labelling and sensitive visualisation of biologically significant molecules. NR is a promising PL nanomaterial that exhibits remarkable photostability and a long emission lifetime. However, fostering widespread applications of nanoruby in molecular imaging requires development of facile and reproducible surface functionalisation procedures.

Silane-based surface functionalisation procedures and covalent conjugation of nanoparticles with biomolecules have found to be an established approach in literature to obtain stable and efficient functionalisation of silica surfaces. Hence, we will extend these approaches to surface functionalise and conjugate NR with proteins such as NeutrAvidin. Details of experimental methodology and the results of functionalising silica nanoparticle (a model system for NR) and NR will be discussed in the following chapters.

References

1. Lakowicz, J.R., *Introduction to fluorescence*, in *Principles of fluorescence spectroscopy*. 1999, Springer. p. 1-23.
2. Jameson, D.M., *Introduction to fluorescence*. 2014: Taylor & Francis.
3. Berezin, M.Y. and S. Achilefu, *Fluorescence lifetime measurements and biological imaging.* Chemical reviews, 2010. **110**(5): p. 2641.
4. Ishikawa-Ankerhold, H.C., R. Ankerhold, and G.P. Drummen, *Advanced fluorescence microscopy techniques—Frap, Flip, Flap, Fret and flim.* Molecules, 2012. **17**(4): p. 4047-4132.
5. Resch-Genger, U., et al., *Quantum dots versus organic dyes as fluorescent labels.* Nature methods, 2008. **5**(9): p. 763-775.
6. Seveus, L., et al., *Time-resolved fluorescence imaging of europium chelate label in immunohistochemistry and in situ hybridization.* Cytometry, 1992. **13**(4): p. 329-338.
7. Denk, W., J.H. Strickler, and W.W. Webb, *Two-photon laser scanning fluorescence microscopy.* Science, 1990. **248**(4951): p. 73-76.
8. Huang, B., M. Bates, and X. Zhuang, *Super-resolution fluorescence microscopy.* Annual review of biochemistry, 2009. **78**: p. 993-1016.
9. Su, Y., et al., *The cytotoxicity of cadmium based, aqueous phase–synthesized, quantum dots and its modulation by surface coating.* Biomaterials, 2009. **30**(1): p. 19-25.
10. Boyer, J.-C. and F.C. Van Veggel, *Absolute quantum yield measurements of colloidal NaYF 4: Er3+, Yb3+ upconverting nanoparticles.* Nanoscale, 2010. **2**(8): p. 1417-1419.
11. Hild, W., M. Breunig, and A. Göpferich, *Quantum dots–nano-sized probes for the exploration of cellular and intracellular targeting.* European Journal of Pharmaceutics and Biopharmaceutics, 2008. **68**(2): p. 153-168.

12. Sreenivasan, V.K., A.V. Zvyagin, and E.M. Goldys, *Luminescent nanoparticles and their applications in the life sciences.* Journal of Physics: Condensed Matter, 2013. **25**(19): p. 194101.
13. Edmonds, A.M., et al., *Nano-Ruby: A Promising Fluorescent Probe for Background-Free Cellular Imaging.* Particle & Particle Systems Characterization, 2013. **30**(6): p. 506-513.
14. Pflitsch, C., R. Siddiqui, and B. Atakan, *Phosphorescence properties of sol–gel derived ruby measured as functions of temperature and Cr3+ content.* Applied Physics A, 2008. **90**(3): p. 527-532.
15. Razali, W.A., et al., *Wide-field time-gated photoluminescence microscopy for fast ultrahigh-sensitivity imaging of photoluminescent probes.* Journal of biophotonics, 2016.
16. Conde, J., et al., *Revisiting 30 years of biofunctionalization and surface chemistry of inorganic nanoparticles for nanomedicine.* Frontiers in chemistry, 2014. **2**: p. 48.
17. Sperling, R.A. and W. Parak, *Surface modification, functionalization and bioconjugation of colloidal inorganic nanoparticles.* Philosophical Transactions of the Royal Society of London A: Mathematical, Physical and Engineering Sciences, 2010. **368**(1915): p. 1333-1383.
18. Veronese, F. and M. Morpurgo, *Bioconjugation in pharmaceutical chemistry.* Il Farmaco, 1999. **54**(8): p. 497-516.
19. Niidome, T., et al., *PEG-modified gold nanorods with a stealth character for in vivo applications.* Journal of Controlled Release, 2006. **114**(3): p. 343-347.
20. Jokerst, J.V., et al., *Nanoparticle PEGylation for imaging and therapy.* Nanomedicine, 2011. **6**(4): p. 715-728.
21. Maldiney, T., et al., *Effect of core diameter, surface coating, and PEG chain length on the biodistribution of persistent luminescence nanoparticles in mice.* ACS nano, 2011. **5**(2): p. 854-862.
22. Veronese, F.M., *Peptide and protein PEGylation: a review of problems and solutions.* Biomaterials, 2001. **22**(5): p. 405-417.
23. Kommareddy, S., S.B. Tiwari, and M.M. Amiji, *Long-circulating polymeric nanovectors for tumor-selective gene delivery.* Technology in cancer research & treatment, 2005. **4**(6): p. 615-625.
24. Yang, Y., et al., *Toxicity and biodistribution of aqueous synthesized ZnS and ZnO quantum dots in mice.* Nanotoxicology, 2014. **8**(1): p. 107-116.
25. Liu, Z., F. Kiessling, and J. Gätjens, *Advanced nanomaterials in multimodal imaging: design, functionalization, and biomedical applications.* Journal of Nanomaterials, 2010. **2010**: p. 51.
26. Razali, W., et al., *Large-scale production and characterization of biocompatible colloidal nanoalumina.* Langmuir, 2014. **30**(50): p. 15091-15101.
27. Buining, P.A., et al., *Preparation of functional silane-stabilized gold colloids in the (sub) nanometer size range.* Langmuir, 1997. **13**(15): p. 3921-3926.
28. Han, Y., et al., *Reverse microemulsion-mediated synthesis of silica-coated gold and silver nanoparticles.* Langmuir, 2008. **24**(11): p. 5842-5848.
29. Darbandi, M., R. Thomann, and T. Nann, *Single quantum dots in silica spheres by microemulsion synthesis.* Chemistry of materials, 2005. **17**(23): p. 5720-5725.
30. Nann, T. and P. Mulvaney, *Single quantum dots in spherical silica particles.* Angewandte Chemie International Edition, 2004. **43**(40): p. 5393-5396.
31. Gerion, D., et al., *Synthesis and properties of biocompatible water-soluble silica-coated CdSe/ZnS semiconductor quantum dots.* The Journal of Physical Chemistry B, 2001. **105**(37): p. 8861-8871.
32. Laurent, S., et al., *Magnetic iron oxide nanoparticles: synthesis, stabilization, vectorization, physicochemical characterizations, and biological applications.* Chemical reviews, 2008. **108**(6): p. 2064-2110.

33. Altavilla, C., *Upconverting Nanomaterials: Perspectives, Synthesis, and Applications*. 2016: CRC Press.
34. Hermanson, G.T., *Bioconjugate techniques*. 2013: Academic press.
35. Hermanson, G.T., *Bioconjugation techniques.* Academic Press, 2008. **10**: p. 0123705010.
36. Veiseh, O., J.W. Gunn, and M. Zhang, *Design and fabrication of magnetic nanoparticles for targeted drug delivery and imaging.* Advanced drug delivery reviews, 2010. **62**(3): p. 284-304.
37. Brancolini, G., et al., *Docking of ubiquitin to gold nanoparticles.* ACS nano, 2012. **6**(11): p. 9863-9878.
38. Strozyk, M.S., et al., *Protein/Polymer-Based Dual-Responsive Gold Nanoparticles with pH-Dependent Thermal Sensitivity.* Advanced Functional Materials, 2012. **22**(7): p. 1436-1444.
39. Ghosh, P.S., et al., *Efficient gene delivery vectors by tuning the surface charge density of amino acid-functionalized gold nanoparticles.* ACS nano, 2008. **2**(11): p. 2213-2218.
40. Guo, S., et al., *Enhanced gene delivery and siRNA silencing by gold nanoparticles coated with charge-reversal polyelectrolyte.* ACS nano, 2010. **4**(9): p. 5505-5511.
41. Foy, S.P., et al., *Optical imaging and magnetic field targeting of magnetic nanoparticles in tumors.* ACS nano, 2010. **4**(9): p. 5217-5224.
42. Kim, C.K., et al., *Entrapment of hydrophobic drugs in nanoparticle monolayers with efficient release into cancer cells.* Journal of the American Chemical Society, 2009. **131**(4): p. 1360-1361.
43. Lacerda, S.H.D.P., et al., *Interaction of gold nanoparticles with common human blood proteins.* ACS nano, 2009. **4**(1): p. 365-379.
44. Deng, Z.J., et al., *Nanoparticle-induced unfolding of fibrinogen promotes Mac-1 receptor activation and inflammation.* Nature nanotechnology, 2011. **6**(1): p. 39-44.
45. Nakajima, N. and Y. Ikada, *Mechanism of amide formation by carbodiimide for bioconjugation in aqueous media.* Bioconjugate chemistry, 1995. **6**(1): p. 123-130.
46. Ju, H., X. Zhang, and J. Wang, *Biofunctionalization of nanomaterials*, in *NanoBiosensing*. 2011, Springer. p. 1-38.
47. Fischer, M.J., *Amine coupling through EDC/NHS: a practical approach.* Surface plasmon resonance: methods and protocols, 2010: p. 55-73.
48. Weissleder, R., et al., *Cell-specific targeting of nanoparticles by multivalent attachment of small molecules.* Nature biotechnology, 2005. **23**(11): p. 1418-1423.
49. Lee, C., et al., *Conjugation of γ-Fe 2 O 3 nanoparticles with single strand oligonucleotides.* Journal of Magnetism and Magnetic Materials, 2006. **304**(1): p. e412-e414.
50. Polo, E., et al., *Plasmonic-driven thermal sensing: ultralow detection of cancer markers.* Chemical Communications, 2013. **49**(35): p. 3676-3678.
51. Roberts, M., M. Bentley, and J. Harris, *Chemistry for peptide and protein PEGylation.* Advanced drug delivery reviews, 2012. **64**: p. 116-127.
52. Farokhzad, O.C., et al., *Nanoparticle-aptamer bioconjugates.* Cancer research, 2004. **64**(21): p. 7668-7672.
53. Li, N. and W.H. Binder, *Click-chemistry for nanoparticle-modification.* Journal of Materials Chemistry, 2011. **21**(42): p. 16717-16734.
54. Sun, E.Y., L. Josephson, and R. Weissleder, *"Clickable" nanoparticles for targeted imaging.* Molecular Imaging, 2006. **5**(2): p. 7290.2006. 00013.
55. Haun, J.B., et al., *Probing intracellular biomarkers and mediators of cell activation using nanosensors and bioorthogonal chemistry.* ACS nano, 2011. **5**(4): p. 3204-3213.
56. Kolb, H.C., M. Finn, and K.B. Sharpless, *Click chemistry: diverse chemical function from a few good reactions.* Angewandte Chemie International Edition, 2001. **40**(11): p. 2004-2021.

57. Krovi, S.A., D. Smith, and S.T. Nguyen, *"Clickable" polymer nanoparticles: a modular scaffold for surface functionalization.* Chemical Communications, 2010. **46**(29): p. 5277-5279.
58. Hein, C.D., X.-M. Liu, and D. Wang, *Click chemistry, a powerful tool for pharmaceutical sciences.* Pharmaceutical research, 2008. **25**(10): p. 2216-2230.
59. Zhu, K., et al., *Quantification of proteins by functionalized gold nanoparticles using click chemistry.* Analytical chemistry, 2012. **84**(10): p. 4267-4270.
60. Brennan, J.L., et al., *Bionanoconjugation via click chemistry: the creation of functional hybrids of lipases and gold nanoparticles.* Bioconjugate chemistry, 2006. **17**(6): p. 1373-1375.
61. Voliani, V., et al., *Multiphoton Molecular Photorelease in Click-Chemistry-Functionalized Gold Nanoparticles.* small, 2011. **7**(23): p. 3271-3275.
62. Zhang, T., et al., *An approach for the surface functionalized gold nanoparticles with pH-responsive polymer by combination of RAFT and click chemistry.* European Polymer Journal, 2009. **45**(6): p. 1625-1633.
63. Wang, S., et al., *Antigen/antibody immunocomplex from CdTe nanoparticle bioconjugates.* Nano letters, 2002. **2**(8): p. 817-822.
64. Hodenius, M., et al., *Magnetically triggered clustering of biotinylated iron oxide nanoparticles in the presence of streptavidinylated enzymes.* Nanotechnology, 2012. **23**(35): p. 355707.
65. Salih, T., et al., *Streptavidin-modified monodispersed magnetic poly (2-hydroxyethyl methacrylate) microspheres as solid support in DNA-based molecular protocols.* Materials Science and Engineering: C, 2016. **61**: p. 362-367.
66. Presnova, G., et al., *Streptavidin conjugates with gold nanoparticles for visualization of single DNA interactions on the silicon surface.* Biochemistry (Moscow) Supplement Series B: Biomedical Chemistry, 2014. **8**(2): p. 164-167.
67. Jiang, Y., et al., *Specific aptamer-protein interaction studied by atomic force microscopy.* Analytical chemistry, 2003. **75**(9): p. 2112-2116.
68. Chaiet, L. and F.J. Wolf, *The properties of streptavidin, a biotin-binding protein produced by Streptomycetes.* Archives of Biochemistry and Biophysics, 1964. **106**: p. 1-5.
69. Tausig, F. and F.J. Wolf, *Streptavidin—a substance with avidin-like properties produced by microorganisms.* Biochemical and biophysical research communications, 1964. **14**(3): p. 205-209.
70. Weber, P.C., et al., *Structural origins of high-affinity biotin binding to streptavidin.* Science, 1989. **243**(4887): p. 85.
71. Dundas, C.M., D. Demonte, and S. Park, *Streptavidin–biotin technology: improvements and innovations in chemical and biological applications.* Applied microbiology and biotechnology, 2013. **97**(21): p. 9343-9353.
72. Alon, R., E.A. Bayer, and M. Wilchek, *Streptavidin contains an RYD sequence which mimics the RGD receptor domain of fibronectin.* Biochemical and biophysical research communications, 1990. **170**(3): p. 1236-1241.
73. Marttila, A.T., et al., *Recombinant NeutraLite Avidin: a non-glycosylated, acidic mutant of chicken avidin that exhibits high affinity for biotin and low non-specific binding properties.* FEBS letters, 2000. **467**(1): p. 31-36.
74. Vermette, P., et al., *Immobilization and surface characterization of NeutrAvidin biotin-binding protein on different hydrogel interlayers.* Journal of colloid and interface science, 2003. **259**(1): p. 13-26.
75. Howarth, M. and A.Y. Ting, *Imaging proteins in live mammalian cells with biotin ligase and monovalent streptavidin.* Nature protocols, 2008. **3**(3): p. 534-545.
76. Torati, S.R., et al., *Protein immobilization onto electrochemically synthesized CoFe nanowires.* International journal of nanomedicine, 2015. **10**: p. 645.

Chapter 3. Experimental Methodology

This chapter describes characterisation techniques used and experimental protocols developed throughout this thesis.

Contents

3.1 Characterisation techniques for photoluminescent nanoparticles

Two characterisation techniques were used to assess the outcomes of functionalisation and bioconjugation experiments. They measure the colloidal properties and infrared absorption of the samples. The principle of these methods and the parameters used for these measurements are detailed in this section.

3.1.1 Dynamic Light Scattering

Dynamic Light Scattering (DLS) is a technique used to measure size of nanoparticles suspended in a colloid[1, 2]. Here, light from a laser source passes through the nanoparticle sample, and the resulting scattered light is collected by the detector. The dynamic fluctuations in the intensity of the light scattered by the nanoparticles undergoing Brownian motion is captured as a time-trace. Since small particles diffuse quicker in a colloid compared to the larger particles, the hydrodynamic diameter of the nanoparticle can be deduced by assessing the dynamic fluctuations using an autocorrelation function[1]. Commercial systems also allow one to easily measure the approximate nanoparticle size distribution in a colloidal suspension.

Zetasizer Nano-ZS, Malvern; USA was used to measure the size and size-distribution of nanoparticles in this thesis. The nanoparticles were dispersed in either water or buffer (mostly phosphate buffered saline; PBS) and transferred to a clear zeta-cell (DTS 1070, Malvern). Material parameters, for example viscosity [0.89cP (water), 0.88cP (PBS)] and refractive index [1.47 (SiO2); 1.33 (water), 1.33 (PBS)], of the solute and the solvent, were fed into the Zetasizer software. All the data presented here is an average of 3 measurements, and only the data that met the "quality criteria" set by the manufacturer is presented. The hydrodynamic diameters used here is the peak position of the number distribution, which emphasises the size range containing largest particle population.

Zeta-potential is a key indicator of the stability of nanoparticle colloids. It is a measure of the electrostatic charge associated with a solid/liquid interface, where most stable nanoparticles are characterised by a high magnitude of the zeta-potential (>30mV)[3]. DLS when used in conjugation with alternating electric field is used to measure the electrophoretic mobility of nanoparticles, from which zeta-potential can be calculated[4]. Zetasizer Nano-ZS was used to measure the zeta-potential of nanoparticles dispersed in either water or buffer. A clear zeta cell containing the suspension was placed into the sample chamber and materials parameters were fed into the Zetasizer software for

measurements. All the data presented here is an average of 3 measurements, and only the data that met the "quality criteria" set by the manufacturer was used. The peak value of the zeta-potential distribution was used for all interpretations. During both size and zeta-potential measurements, optimising the sample concentration and/or brief sonication of the sample solution usually improved quality and reliability of data.

3.1.2 Fourier Transform Infrared spectroscopy

Fourier transform infrared (FTIR) spectroscopy is a technique for identifying the presence of particular chemical bonds, which is commonly used to infer the presence of functional groups or molecules in a sample. An FTIR spectrum is obtained by passing infrared radiation through a sample and determining the fraction of the absorbed (or transmitted) radiation at a particular energy. Since the energy depends on the vibrational modes of specific chemical bonds, FTIR spectroscopy provides qualitative analysis of different chemical groups in a material[5].

A Nicolet^{TM} iS5 FTIR spectrometer (Thermo Fisher; USA) was used to acquire spectra before and after functionalisation/conjugation of nanoparticles. Air-dried samples were placed directly on the attenuated total reflectance (ATR) crystal window, and compressed using a tip to ensure contact with the ATR crystal. Scanning parameters, for example, the spectral range (500 cm^{-1}- 4000 cm^{-1}) were fixed, and the spectrometer was programmed to acquire % transmission at room temperature. All measurements were accompanied by background spectra (where no sample was used) for background subtraction. This eliminated signals arising from spectrometer and the environment.

3.2 Development of silane-functionalised photoluminescent nanoparticles

Silane-based chemistries were tested to functionalise silica nanoparticles (SNP) (sicastar®-greenF; Micromod, Germany) and silica-coated ruby nanoparticles (SiNR, prepared in-house). The reagents used were a mixture of silane-PEG reagents comprising of (i) a monofunctional poly-ethylene glycol (PEG), with silane on one end and inert methyl group on the other (silane-mPEG; Laysan Bio, USA; MW 2000), and (ii) a heterobifunctional PEG, with silane at one of the terminals and either of the three chemical groups described below at the second terminal (silane-PEG-X; Nanocs, USA; MW 3400). A range of concentrations of the net silane-PEG reagent mixture (0 to 100-mM) were studied for functionalising SNP efficiently with reactive chemical groups, in addition to maintaining its size and stability. The fraction of silane-PEG-X in the total silane-PEG

reagent mixture was varied (0.1, 1, 3, 20%) and optimised. MilliQ (MQ) water was used as a solvent in all the functionalisation steps, except otherwise mentioned. Different protocols were developed for the three-different silane-PEG-X reagents: silane-PEG-COOH (PG2-CASL-3k; Nanocs, USA; MW 3400), silane-PEG-NHS (PG2-NSSL-3k; Nanocs, USA; MW 3400) and silane-PEG-azide (PG2-AZSL-3k; Nanocs, USA; MW 3400). They introduced one of the following three functional groups onto the SNP surface, respectively: COOH (carboxylic acid), NHS (N-hydroxysuccinimide ester) and azide (N_3). These groups allowed conjugation of the functionalised SNP with the protein NeutrAvidin (NA) (31000; ThermoFischer Scientific, USA; 10 mg) using either of the three specifically designed conjugation reactions, which is discussed in the next section.

The following protocol was formulated for functionalising SNP based on a number of preliminary experiments, and it yielded reproducible results:

1. Centrifuge the 5 mg of SNP at 16000 g for 5 mins. Discard the supernatant.
2. Resuspend the SNP pellet in 300 µL MQ water.
3. Wash the SNP twice (repeat step 1 and step 2) and finally resuspend the pellet into 100 µL MQ water.
4. Add silane-mPEG and silane-PEG-X dissolved in water to the SNP solution, while maintaining the net silane-PEG reagent concentration at 30-mM or 60-mM. The fraction of silane-PEG-X in the silane-PEG reagent mixture was varied between 0.1-20%.
5. Incubate the mixture overnight at 40°C.
6. Wash the functionalised SNP by centrifuging at 13500 g for 5 mins and resuspend the pellet in 300 µL MQ water.
7. Repeat the washing step five times (in total) to remove excess and loosely bound silane-PEG reagents. At last, redisperse the functionalised SNP into 100 µL MQ water for further conjugation with protein, NeutrAvidin (NA).

Note 1: Use dimethyl sulfoxide (DMSO; 276855; Sigma Aldrich, USA; anhydrous ≥99.9%) instead of water in steps 4-7 when using silane-PEG-NHS, because NHS hydrolyses rapidly when contacted with moisture.

Note 2: All moisture sensitive steps were carried out inside a nitrogen gas-purged Atmos Bag (Sigma Aldrich).

This procedure yielded functionalised silica nanoparticles, referred to as SNP-PEG-COOH, SNP-PEG-NHS or SNP-PEG-azide.

SiNR was functionalised only using silane-PEG-azide. For this, 0.16 mg of SiNR was incubated with 200 µL of an aqueous solution containing silane-mPEG and silane-PEG-azide at desired concentration ratio (0.1 – 10 %), while maintaining the final concentration at 60-mM. The rest of the reaction was carried out as described for SNP, giving rise to SiNR-PEG-azide.

3.3 Development of conjugated nanoparticles with NeutrAvidin

The functionalised nanoparticles were conjugated with NA. Three covalent conjugation methods were designed based on the three functional groups introduced on the nanoparticle surfaces.

3.3.1 Method A: Using carbodiimide chemistry

A covalent reaction that links the COOH group on the surface of SNP-PEG-COOH to NH_2 (amine) groups in NA molecules was designed to yield a stable and functional SNP-NA conjugate. This reaction requires pre-activation of the COOH group, which was performed using *N*-[3-Dimethylaminopropoyl]-*N'*-ethyl carbodiimide hydrochloride (EDC; Sigma Aldrich) and N-hydroxysuccinimide (NHS; Sigma Aldrich). The following bioconjugation reaction was formulated based on preliminary experiments, and yielded reproducible results:

1. Centrifuge 200 µL of SNP-PEG-COOH (50 mg/mL) at 13500 g for 5 mins and resuspend the pellet in 300 µL MES buffer (10-mM; pH 6.1). Note: Low pH increases the efficiency of activating the COOH groups [6].
2. Prepare fresh solutions of EDC and NHS, both 5 mg in 300 µL of MES buffer respectively.
3. While gently mixing, first add EDC (5 mg/mL) and then NHS (5 mg/mL) to the SNP-PEG-COOH solution, and make the final volume to 1 mL with MQ water. Continue the reaction under stirring for 15 mins at room temperature. Stirring was identified to be necessary to avoid aggregation during this step.
4. Centrifuge the activated SNP-PEG-COOH at 13500 g for 5 mins, and resuspend in 200 µL MES buffer. Repeat the washing step twice to remove the excess EDC and NHS. Suspend the activated SNP-PEG-COOH in PBS (10 mM; pH 7.2) and immediately proceed to the next step.

5. While gently mixing, add 20-µM NA solution (stock: 0.33-mM) to the activated nanoparticle solution and adjust the volume to 200 µL with PBS. Note: PBS (pH 7.2) mimics biological fluids and maintains protein structure and biological activity [7].
6. Continue the reaction under stirring using a rotary mixer for 2 hours at room temperature. Stirring is necessary to avoid agglomeration and to achieve uniform reaction with NA.
7. Quench residual activated COOH groups with a final concentration of 10-mM ethanolamine (EA) for 15 mins at room temperature. Note: This blocking step is expected to prevent subsequent non-specific interactions during biological applications [6].
8. Wash by centrifuging the SNP-NA conjugates at 13500 g for 5 mins, and resuspending the pellet in 200 µL of PBS. Repeat the washing step five times (in total) to remove excess and loosely bound NA.
9. Store the obtained SNP-NA conjugate in 200 µL PBS, at 4°C
10. For a negative control, follow the same procedure, but without EDC and NHS reagents, to test covalent nature of the SNP-NA conjugation.

3.3.2 Method B: Using N-hydroxysuccinimide (NHS) ester chemistry

A covalent reaction that links the reactive NHS ester group on the surface of SNP-PEG-NHS to the NH_2 group in NA molecules was designed, and expected to yield a stable SNP-NA conjugate. The following bioconjugation reaction was formulated based on preliminary experiments, and yields reproducible results:

1. Centrifuge 200 µL of SNP-PEG-NHS (50 mg/mL) at 18500 g for 5 mins and discard the DMSO supernatant from the functionalisation reaction.
2. Immediately prior to the reaction, resuspend the pellet in borate buffer (10 mM; pH 8.3). Note: For the NHS ester to amine condensation reaction, a pH value of 7.2-8.5 is most desirable [6].
3. While mixing gently, add 20-µM NA solution (0.33-mM) to the activated SNP solution and adjust the volume to 200 µL with borate buffer.
4. Prepare a control sample as described above, except addition of 50-mM ethanolamine (EA) between steps 2 and 3, thereby quenching the NHS-ester groups and preventing conjugation to NA starting in step 3. This is to confirm the covalent conjugation between SNP and NA.

5. Continue the reaction under stirring using a rotary mixer for 3 hours at room temperature. Stirring is necessary to avoid agglomeration and for uniform reaction with NA.
6. To remove unbound excess NA, wash the sample thrice with borate buffer (pH 9) by centrifuge at 13500 g for 5 mins. Resuspend the final pellet in 200 µL borate buffer (pH 8.3). Sonicate mildly to suspend the NA (or EA or BSA) -conjugated SNP uniformly in the Borate buffer.
7. Treat the SNP-NA conjugate (or the two controls) with a final concentration of 50-mM EA for 1 hour at room temperature, to quench the residual active NHS.
8. Centrifuge the SNP-NA conjugates (or controls) at 13500 g for 5 mins, and resuspend in 200 µL Borate buffer (pH 8.3). Repeat the washing step five times (in total) to remove excess and loosely bound NA.
9. Finally, store the SNP-NA conjugates in 200 µL borate buffer, at 4°C.

3.3.3 Method C: Using copper-free click chemistry

In this approach, a NHS ester functionalized Dibenzocyclooctyne (DBCO-NHS ester; Nanocs, USA) was employed to first incorporate an alkyne moiety(-ies) into NA. Then, a covalent reaction that links the reactive azide group on SNP-PEG-azide to the alkyne group introduced into the NA molecule was designed, yielding a stable SNP-NA conjugate. The following two step bioconjugation reaction was formulated based on preliminary experiments, and yielded consistent results.

Step 1: Activation of NeutrAvidin (NA) with DBCO-NHS ester

1. Freshly prepare 10-mM DBCO-NHS ester solution in DMSO.
2. Under gentle vortexing, mix 4-fold molar excess of DBCO-NHS ester with 0.2-mM NA solution in PBS (10 mM; pH 7.2).
3. Continue the reaction under stirring using a rotary mixer for 1 hour at room temperature.
4. Equilibrate a desalting column (ThermoFischer Scientific; 7K MWCO) with PBS.
5. Remove the excess DBCO reagent by eluting the sample through the desalting column. Collect the eluate containing DBCO-NA in a fresh vial and store at 4°C.
6. Prepare a negative control sample to test covalent binding by using DBCO-NHS that was pre-quenched with 50-mM ethanolamine (EA) by overnight incubation, resulting in DBCO-EA. React the DBCO-EA conjugate with NA, and follow the steps described above.

Step 2: Click reaction of DBCO-NeutrAvidin with SNP-PEG-azide

1. Centrifuge 200 µL of SNP-PEG-azide (50 mg/mL) at 13500 g for 5 mins and resuspend the pellet in PBS.
2. While mixing gently, add 16 µL of 0.12-mM DBCO-NA (or control) to the nanoparticle solution.
3. Continue the reaction under stirring for 3 hours at room temperature.
4. Centrifuge the SNP-NA conjugate at 13500 g for 5 mins, and resuspend the pellet in 200 µL PBS. Repeat the washing step five times (in total) to remove excess and loosely bound DBCO-NA.
5. Store the SNP-NA conjugates in 200 µL PBS at 4°C.
6. Test the covalent binding by three controls. First control is described above by using quenched DBCO-EA. Prepare a second control by using functionalised SNP-PEG instead of SNP-PEG-azide for the conjugation reaction with DBCO-NA. Prepare a third control by conjugating SNP-PEG-azide with NA, instead of DBCO-NA.

The methods based on click chemistry, developed and described in Sections 3.2 and 3.3 were extended to conjugate SiNR with NA. For the reaction, 0.16 mg of SiNR-PEG-azide was mixed with 16 µL of 0.12-mM DBCO-NA (or control). The rest of the reaction was the same as described for SNP functionalisation.

3.4 Fluorescence-based biotin binding assay

The presence of NA bound on the surface of SNP was measured using a fluorescence-based assay using a dye-labelled biotin (Promofluor-555P, Biotin; Promokine; Germany). Measurement of fluorescence intensity of Promofluor-biotin bound to SNP or SiNR indirectly reported on the presence of functional NA on the nanoparticle surface. This intensity, when normalised and expressed as a percentage of fluorescence of SNP or SiNR, is a quantitative measure of ratio of NA molecules bound to SNP or SiNR. A negative control to test the validity of the assay was also developed by using excess of unlabelled biotin, which quenched the specific biotin-binding sites in the sample.

SNP-NA conjugates (or controls) from each of the three covalent chemistries were reacted with 1-µM Promofluor-biotin. The samples were washed by centrifuging at 13500g for 5 mins and resuspended in PBS (pH 7.2). The washing step was repeated five times (in total) to remove excess and loosely bound biotin label, diluted and analysed using a Fluorolog

Tau 3 spectrofluorometer (JY Horiba). The obtained spectra were corrected using baseline values obtained with PBS or water. The intensities at the peak of the emission spectra of Promofluor-Biotin, SNP and SiNR were used for normalisation and analysis. Statistical comparisons between groups (samples and the various controls) were made using a two-way Students T-test with a value of $P < 0.05$ being considered significant for all comparisons.

3.5 Labelling and imaging of opioid receptor in fixed and live cells

The developed SNP-NA and SiNR-NA (and controls) were used to label μ-opioid receptors (MOR) in AtT20 cells that stably and heterologously expressed either N-terminally HA-epitope tagged human mu-opioid receptors (HA-hMOR) or N-terminally FLAG-epitope tagged mouse mu-opioid receptors (FLAG-mMOR). The FLAG-mMOR was a negative control, because the antibody used to label the receptors were targeted against the HA-epitope. The cell lines were developed by Prof. Mark Connor, Macquarie University as described previously[8, 9].

Cells were plated in 8-chambered slide (Thermofisher Scientific) and grown overnight in an incubator maintained at 37 °C and 5% CO2 in DMEM supplemented with 10% FBS, Penicillin/Streptomycin and 100 μg. mL^{-1} Hygromycin (selection antibiotic for HA tagged receptor-expressing cells) or 300 μg. mL^{-1} G418 (selection antibiotic for FLAG-tagged receptor-expressing cells). Biotinylated anti-HA antibody (Covance) were used to target the HA-hMOR to which the SNP-NA conjugates or SiNR-NA conjugates (or controls) were targeted for specific labelling.

The labelling procedure was different for labelling in fixed and live cells. For labelling in fixed cells, the cells were first fixed with 3.7% paraformaldehyde in PBS for 20 min. The fixed cells were blocked with 1% bovine serum albumin (BSA) solution prepared in Lebovitz L15 medium (hereafter referred to as serum starve medium) for 1 hr at room temperature. For labelling in live cells, the cells were equilibrated to room temperature for 15 mins and subsequently incubated in serum starve medium for 20 mins at room temperature.

Biotinylated anti-HA antibody was diluted 500 times in serum starve medium, added to the cells and incubated for 1 hour at room temperature. The samples were rinsed three times with serum starve medium. SNP-NA (100 μg/mL) or SiNR-NA (100-150

µg/mL)) were prepared in serum starve medium, added to the cells, and incubated at room temperature for 10 mins under gentle rocking.

In fixed cell labelling, the cells were washed once with serum starve medium and twice with PBS, before mounting for fluorescence microscopy. In live cell labelling, the cells were rinsed once with serum starve medium, and twice with PBS, and fixed with 3.7% paraformaldehyde in PBS for 20 mins. The cells were washed twice with PBS before mounting for fluorescence microscopy.

3.5.3 Microscopy

Imaging of opioid receptors in cells using SNP were carried out using Leica SP5 inverted confocal laser scanning microscope, with Argon 488 nm excitation using a 63x oil immersion objective. Z-stacks of the images were acquired at 1-µm depth resolution and projected based on maximum pixel basis for visualisation.

Images of NR labelled receptors were acquired using a wide-field time gated imaging microscope developed in-house, and described elsewhere[10]. Briefly, a 532-nm laser was used to uniformly excite the sample using a 100x oil-immersion objective with a power density of approximately 250 $W.cm^{-2}$. The generated NR fluorescence was collected using an EMCCD (Andor). The laser and the camera were timed using an external pulse generator. Time-gated acquisition was achieved by starting the camera acquisition 10 µs past the end of each laser pulse. Images were acquired at different z-planes by manually translating the sample. Images were projected using a maximum pixel algorithm onto a single plane for visualisation. These images were analysed to detect the number of particles labelling per cell both in sample and control groups using Trackmate, an open source Fiji plugin for the automated, semi-automated, and manual tracking of single particles [11]. Statistical comparisons between groups (sample and controls) were made using a two-way Students T-test with a value of $P < 0.05$ being considered significant for all comparisons.

References

1. Pecora, R., *Dynamic light scattering: applications of photon correlation spectroscopy*. 2013: Springer Science & Business Media.
2. Dahneke, B.E., *Measurement of suspended particles by quasi-elastic light scattering*. 1983: John Wiley & Sons.
3. Clogston, J.D. and A.K. Patri, *Zeta potential measurement.* Characterization of nanoparticles intended for drug delivery, 2011: p. 63-70.

4. Hunter, R.J., *Zeta potential in colloid science: principles and applications*. Vol. 2. 2013: Academic press.
5. Doyle, W.M., *Principles and applications of Fourier transform infrared (FTIR) process analysis.* Process control and quality, 1992. **2**: p. 50.
6. Hermanson, G.T., *Bioconjugate techniques*. 2013: Academic press.
7. Costantino, H.R. and M.J. Pikal, *Lyophilization of biopharmaceuticals*. Vol. 2. 2004: Springer Science & Business Media.
8. Knapman, A., M. Santiago, and M. Connor, *Buprenorphine signalling is compromised at the N40D polymorphism of the human μ opioid receptor in vitro.* British journal of pharmacology, 2014. **171**(18): p. 4273-4288.
9. Knapman, A., et al., *A continuous, fluorescence-based assay of μ-opioid receptor activation in AtT-20 cells.* Journal of biomolecular screening, 2013. **18**(3): p. 269-276.
10. Razali, W.A., et al., *Wide-field time-gated photoluminescence microscopy for fast ultrahigh-sensitivity imaging of photoluminescent probes.* Journal of biophotonics, 2016. **9**(8): p. 848-858.
11. Tinevez, J.-Y., et al., *TrackMate: An open and extensible platform for single-particle tracking.* Methods, 2017. **115**: p. 80-90.

Chapter 4. Results on functionalising Fluorescent Silica Nanoparticles

This chapter forms a test-bed to develop a robust and reproducible method for conjugating silica-coated nanoruby (SiNR) with NeutrAvidin (a streptavidin analogue). Fluorescent silica nanoparticles (SNP) were used as a model nanoparticle for SiNR. The developed protocols include a functionalisation reaction, where chemical functional groups are first introduced on the SNP surface, and a conjugation reaction where NA is covalently reacted to the introduced functional groups. Three strategies of functionalisation and conjugation were designed and tested, where only the click-chemistry based method yielded a stable, functional and reproducible SNP-NeutrAvidin (SNP-NA) conjugate. The conjugate was demonstrated to be useful for specific cell-labelling and imaging applications. The developed method was implemented for conjugating SiNR with NeutrAvidin, and addressed in the next chapter.

Contents

4.1 Introduction

Fluorescent SNP was chosen as a model system to develop conjugation protocols for SiNR due to several reasons. Firstly, synthesis of SiNR is currently time-consuming and is not suitable for testing and optimising conjugation reactions, where large quantities of material is needed. Thus, a readily available model nanoparticle that has similar size and surface properties was desired. SNP is commercially available in several sizes, including 100 nm, and with various surface functional groups, including hydroxyl, which match the properties of SiNR. SNP is also available with various fluorescent dopants, and is relatively inexpensive. Moreover, SNP is a long-standing bio-safe nanomaterial in its own right, and the protocols developed may be useful for its own applications in imaging and sensing[1, 2]. Therefore, SNP represented a cost-effective and readily available model that mimicked properties of in-house developed SiNR for testing and developing conjugation strategies. Commercially-procured SNPs were thoroughly characterised prior to carrying out functionalisation and conjugation reactions.

4.2 Characterisation of SNP

The physicochemical and photophysical properties of SNP were characterised in terms of their size, zeta potential, FTIR and fluorescence spectra. The hydrodynamic diameter of the SNP suspended in water was measured by Dynamic Light Scattering (DLS, Section 3.1.1) to be ≈100 ± 2 nm, as specified by the manufacturer (Micromod). The zeta potential of SNPs, suspended in water, was ≈ -38 ± 1 mV in agreement with the known isoelectric point of ≈ 3[3]. The FTIR spectra [Figure 4.3 (a)] also showed peaks at 3400-3500 cm^{-1} corresponding to Si-OH stretching on the nanoparticle surface, in addition to the strong band in 954-1094 cm^{-1} region assigned to the Si-O-Si asymmetric stretching vibrations[4]. Taken together, these confirmed the hydroxylated surface of SNR, per the manufacturer's specification. Fluorescence of SNP was measured using a Spectrofluorometer to confirm the specifications of the manufacturer (Figure 4.1). Next, SNPs were functionalised to introduce reactive functional groups on their surface.

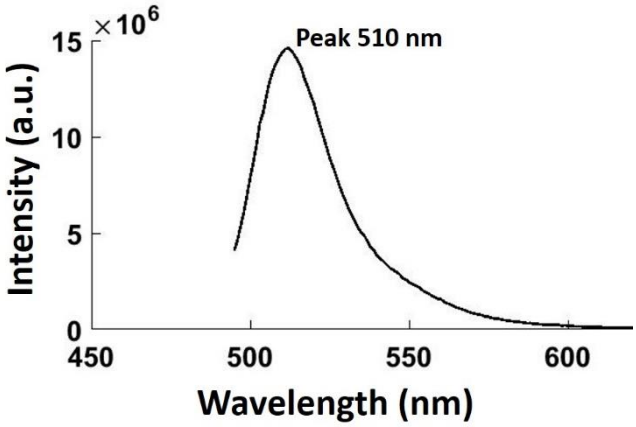

Figure 4.1 Emission spectra of fluorescent SNP (sicastar®-greenF) sample under excitation at 485 nm

4.3 Silane-based surface functionalisation

Silane-based chemistry described in the literature is a straightforward and efficient approach for covalently modifying surfaces harbouring hydroxyl moieties, including silica[5]. In this process known as a silanization reaction, a silane reagent X-Si-O-(R) is hydrolysed in water to form a silanol X-Si-OH, which spontaneously cross-links with -OH groups on the silica, resulting in a strong covalent immobilisation of -X group on the silica surface[6], where X denotes a reactive group, such as COOH, NHS, azide, etc., to allow subsequent covalent conjugation of a protein molecule.

Colloidal stability of nanoparticles in physiologically relevant solvents, such as PBS, critically important for applications in Life Sciences, represents another functionalisation goal. The surface-engineered electrostatic repulsion keeps nanoparticles stable in aqueous solution but fails to maintain the stability in salt-containing buffers, due to the charge screening. Introducing steric stabilisation using polymers, such as polyethylene glycol (PEG) and the other block polymers is a common approach to ameliorate this problem[7].

We combined two benefits of the functionalisation by using silane-reagents, which had both PEG and a reactive functional group (i.e., silane-PEG-X). The first goal of the next section is to present the optimisation of the concentration of silane-PEG-X reagents to efficiently passivate 100-nm SNP. This reaction was carried out by using a non-reactive reagent silane-mPEG (where X is an inert methyl group). Next, by replacing a small

percentage of silane-mPEG with reactive species, one can control the number of reactive functional groups (X) on the SNP surface. Therefore, optimising the ratio of silane-mPEG and reactive silane-PEG-X to introduce sufficient functional terminals without compromising colloidal stability, represents the second goal of the next section.

4.3.1 Optimisation of concentration of silane-PEG reagents

A range of concentrations of silane-mPEG (1, 3, 10, 30, 100 mM) was used to maximise the surface coating of SNP (Section 3.2) with PEG. Figure 4.2 shows the size and zeta potential of SNP reacted with silane-mPEG versus its concentrations. The size for the SNP was observed to be around 116 ± 2 nm, while the zeta potential was found to be around 33 ± 2 mV, irrespective of the reagent concentration. This suggested that the surface modification by silane-mPEG had little influence on the size and the zeta potential of SNP in water.

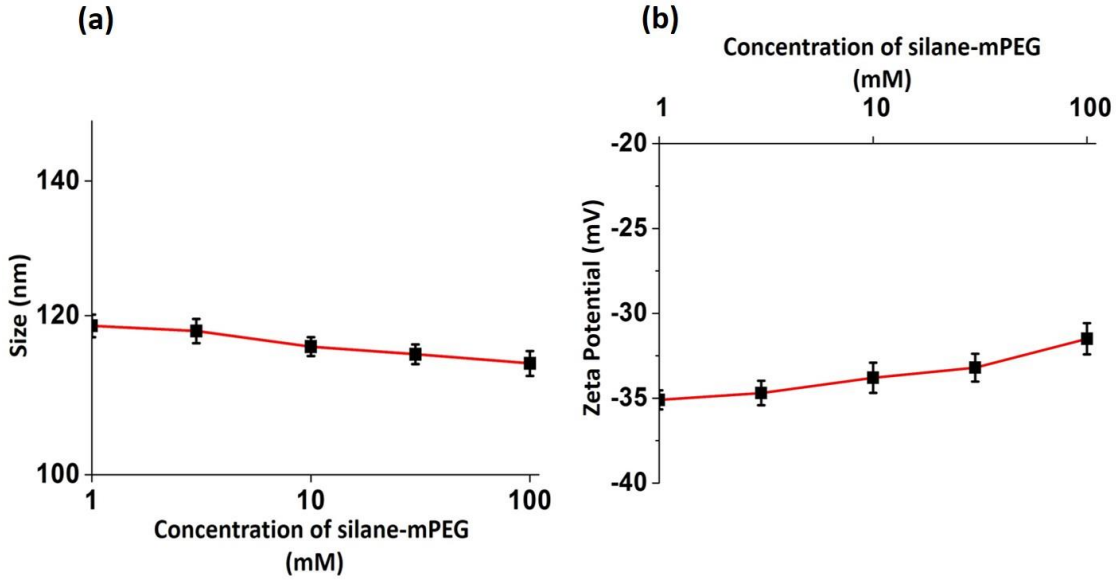

Figure 4.2 Variation of the (a) hydrodynamic size (diameter) and (b) zeta potential of PEG-functionalised SNP (SNP-PEG) depending on the concentration of silane-mPEG reagent used, as measured by DLS.

In order to obtain quantitative data on the presence of PEG, the functionalised samples were analysed using infrared (FTIR) spectroscopy. The spectra of the PEG-coated SNP revealed absorption peaks at 2885 and 2950 cm^{-1} corresponding to characteristic peaks of PEG (C-H stretching) [Figure 4.3 (a)]. PEG peak intensity at 2900 cm^{-1} showed an increasing trend with the concentration of silane-mPEG, saturating at ~ 60 mM [Figure 4.3

(b)]. Therefore, a silane-PEG reagent concentration range of 30 – 60 mM was used for the functionalisation throughout this thesis.

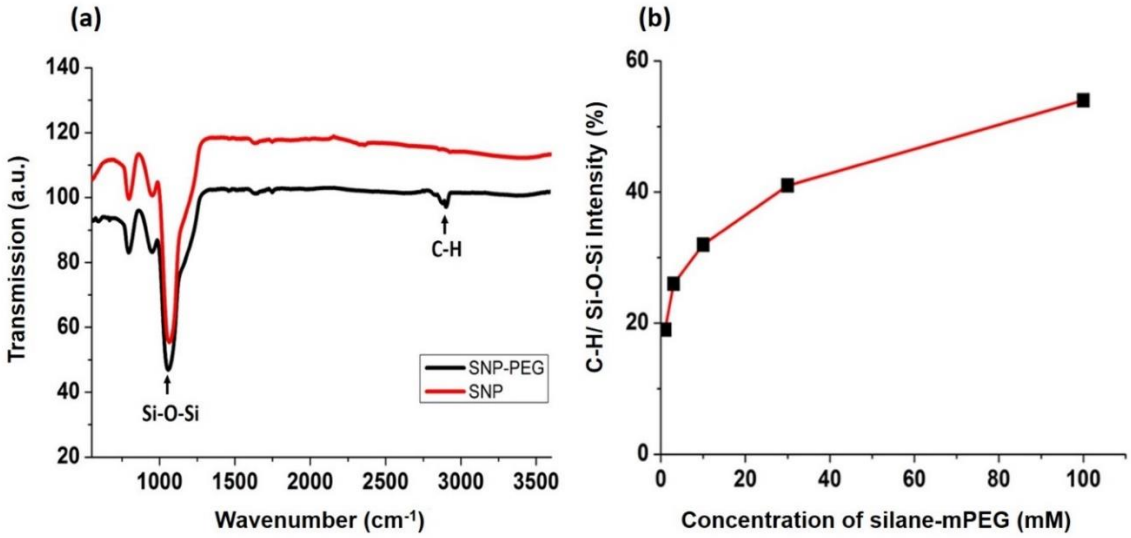

Figure 4.3 FTIR spectroscopy based characterisation of bare SNP and that functionalised with different concentrations (1mM to 100 mM) of silane-mPEG (SNP-PEG) (a) FTIR spectra of SNP and SNP-PEG normalised to Si-O-Si stretching (SNP) peak, and (b) intensity of C-H stretching (from PEG) normalised to Si-O-Si stretching (SNP) peak.

4.3.2 Optimisation of the concentration ratio between silane-PEG reagents

The fraction of silane-PEG-X in the next silane-PEG reagent mixture was varied from 1 to 100% to identify a range, which introduced sufficient number of functional groups on the SNP without compromising the colloidal properties (Section 3.2). This was characterised based on the size and zeta potential of SNP after functionalisation. Figure 4.4 presents the size and zeta potential of the samples functionalised with silane-PEG reagents as a function of the silane-PEG-COOH content. The data shows a dramatic increase in the hydrodynamic diameter of up to 1 μm, when the percentage of silane-PEG-COOH exceeded 20-40% [Figure 4.4 (a)]. The trend in the zeta potential [Figure 4.4 (b)], revealed that the aggregation threshold of -30 mV[8] was reached at 30% of the COOH reactive groups. FTIR spectroscopy was used to quantify the COOH groups, but the peaks at 1710-1780 cm^{-1} (C=O stretching) were not significant, perhaps due to the low abundance of this group per silane-PEG-COOH molecule.

SNP was functionalised using three silane-PEG-X reagents: silane-PEG-COOH, silane-PEG-NHS (N-hydroxysuccinimide ester) and silane-PEG-azide using a protocol

described in section 3.2. The ratio of silane-PEG-X to silane-mPEG was kept below 20% for all these functionalisation reactions to prevent aggregation.

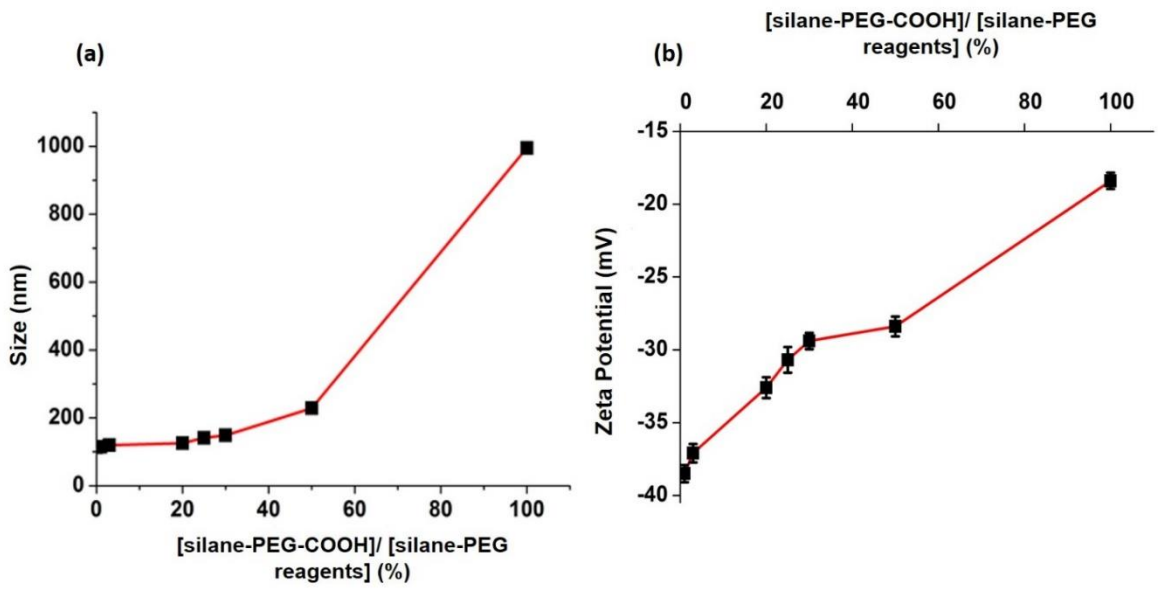

Figure 4.4 Colloidal properties, (a) hydrodynamic size (diameter) and (b) zeta potential, of SNP functionalised with a mixture of silane-PEG-COOH and silane-mPEG, as measured by DLS. The fraction of silane-PEG-COOH in the silane-PEG reagent mixture was varied, as denoted by percentage values.

4.4 Covalent conjugation of SNP with NeutrAvidin

The three functional groups (COOH, NHS or azide) introduced on the SNP surface was used to conjugate NA molecules using its intrinsic amine groups. The conjugation strategy and results from these experiments are described below.

4.4.1 Carbodiimide chemistry

4.4.1.1 Chemistry and Strategy

The first method we tested was to use COOH surface groups to covalently link with amine groups in NA molecule, yielding a stable SNP-NeutrAvidin conjugate (Figure 4.5). The reaction was optimised based on various experimental parameters (Section 3.3.1), including concentration of catalysts- EDC and NHS (data not shown), molar ratio of silane-PEG-COOH to silane-mPEG (1, 3 and 20 %) to change the number of reactive terminals, concentration of total silane-PEG reagents to reduce the non-specific binding, and controls (absence of EDC/NHS) to test the covalent nature of the conjugation.

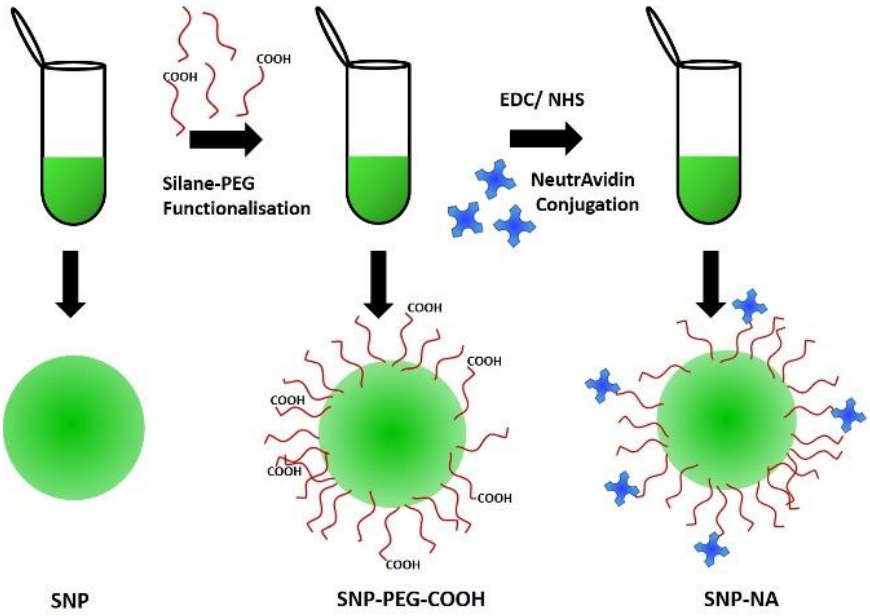

Figure 4.5 Schematic diagram of SNP functionalisation with a mixture of silane-PEG-COOH and silane-mPEG, followed by NA conjugation using carbodiimide chemistry.

4.4.1.2 Characterisation by DLS

Table 4.1 summarises the size and zeta potential values of COOH functionalised SNP and subsequently conjugated to NA, for various concentrations of the reagents. The use of 20% silane-PEG-COOH resulted in an increase of the hydrodynamic diameter from 126 nm before NA conjugation to ≈ 496 nm after the conjugation. The increased size and the sedimentation observed by visual inspection of the sample suggested severe aggregation. The presence of many NA molecules per SNP may be the reason for this aggregation, since the use of 1 and 3 % silane-PEG-COOH reagents led to stable SNP-NA conjugates. The biotin-binding function of these conjugates were characterised using a fluorescence-based binding assay, which relied on a fluorescently modified biotin (Promofluor-biotin).

Samples	Amount of [silane-PEG-COOH]/ [silane-PEG reagent] (%)	Size (nm)	Zeta (mV)	Size (nm)	Zeta (mV)
		30 mM silane-PEG reagents		60 mM silane-PEG reagents	
SNP-PEG-COOH	20	126	-7	-	-
	3	119	-6	120	-7
	1	114	-6	115	-8
SNP-NA	20	496	-5	-	-
	3	123	-6	124	-7
	1	116	-6	118	-7

Table 4.1: Characterisation of SNP functionalised with COOH groups, and subsequently conjugated with NA with varying concentrations and ratios of silane-PEG reagents as shown. 30mM and 60mM are the combined concentration of silane-PEG-COOH and silane-mPEG.

4.4.1.3 Characterisation by Biotin Binding

A biotin binding assay was designed to confirm the presence and biological function of covalently conjugated NA on the surface of SNP (Section 3.4).

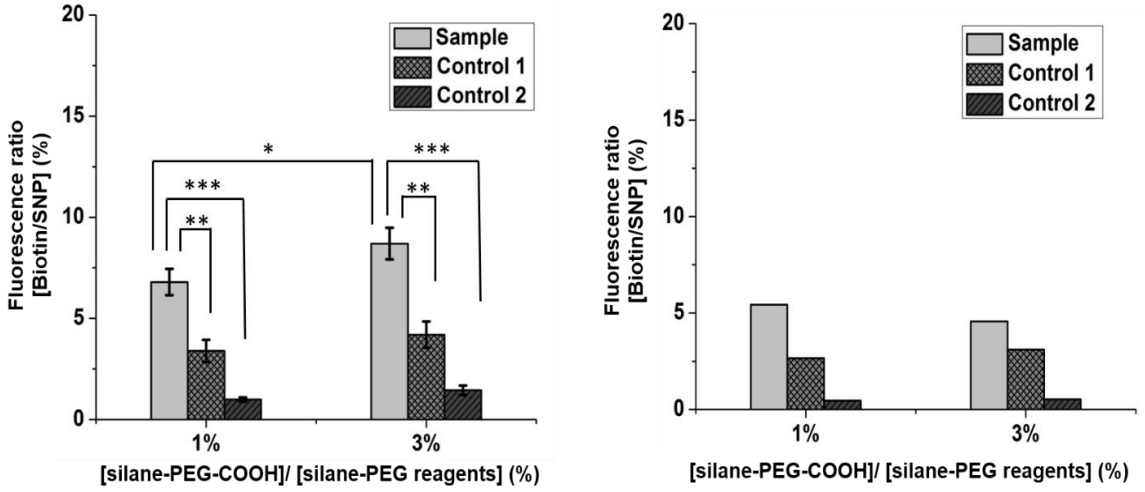

Figure 4.6: Biotin binding, as measured by a fluorescence based assay, for SNP functionalised (a) with 30 mM silane-PEG reagents containing varying molar fraction of

silane-PEG-COOH, followed by conjugation with NA and (b) with 60 mM silane-PEG reagents, followed by conjugation with NA, and with 10-fold less Promofluor-biotin for the assay. Control 1 corresponds to reaction carried out without EDC and NHS to test the covalent nature of conjugation, and Control 2 corresponds to biotin binding assay carried out on COOH-functionalised SNP to measure non-specific binding. *, ** and *** indicates *P*-value < 0.01, < 0.001 and < 0.0001 respectively analysed using a two-way Students T-test.

Figure 4.6 (a) shows the SNP functionalised with 3% silane-PEG-COOH (30 mM total silane-PEG reagent) had the greater biotin binding efficiency (≈ 9 %), as compared to ≈ 6 % for the 1% silane-PEG-COOH sample, suggesting that 3% silane-PEG-COOH SNP sample had the higher number of conjugated NA molecules. However, there was a concomitant increase in biotin binding in Control 1 (≈ 4 %), which was prepared without EDC/NHS in the reaction. This suggested that a significant fraction of NA molecules were physically adsorbed on the surface, rather than being covalently bound. We also observed that Promofluor-biotin also binds non-specifically by itself to SNP-PEG-COOH even in the absence of NA (data not shown). Therefore, we tested if reducing the concentration of dye-biotin biotin by ten-fold (1 μM → 0.1 μM) would result reduced non-specific binding. While we did observe a reduction in non-specific binding, the fluorescence intensity for the sample (≈ 5.5 %) also reduced slightly [Figure 4.6 (b)].

These results show that carbodiimide based conjugation chemistry results in attachment of NA on COOH-functionalised SNP nanoparticles, but only about half of the bound NA are covalently attached. This also suggests that the SNP-PEG-COOH also has propensity for adsorbing other proteins, and can result in high degree of non-specific binding and aggregation. We questioned if the efficiency and specificity of covalent conjugation reaction can be improved by using more reactive or specific functional groups instead of COOH.

4.4.2 NHS ester chemistry

4.4.2.1 Chemistry and Strategy

NHS-esters have high reactivity to amine groups, and can avoid several steps in comparison to the carbodiimide chemistry. NHS ester functionalised SNP was used to covalently immobilise NA in a single step reaction, as schematised in Figure 4.7. Since NHS moieties hydrolyse within minutes in the presence of water, all steps of

functionalisation and conjugation using NHS ester were carried out in dimethyl sulfoxide (DMSO).

The chemistry was optimised for several parameters (Section 3.3.2), including buffer to improve the efficiency of the reaction, molar ratio of silane-PEG-NHS to silane-mPEG (3 %, 1%, 0.3 %), concentration of NA to reduce non-specific binding, and controls to test for the covalent nature of the conjugation. Similar reactions were carried out for controls, where the reactive NHS group on the SNP surface was inactivated either ethanolamine (Control 1) prior to addition of NA. Another control was carried out where the inactivation was performed with BSA, but the results are not different from that of Control 1 and not presented. The biotin-binding activity in this control would result from adsorbed NA or non-specific biotin-binding. NHS-functionalised SNP (without NA) treated with fluorescent biotin served as Control 2, where any biotin binding would indicate non-specific biotin-binding. All the conjugates (and controls) were also characterised by measuring size and zeta potential by DLS.

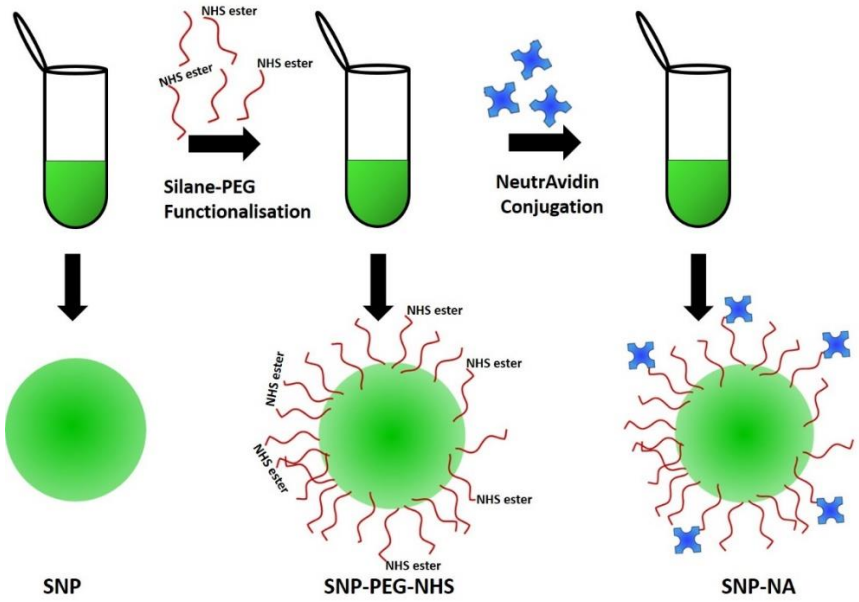

Figure 4.7 Schematic diagram of SNP functionalisation with a mixture of silane-PEG-NHS ester and silane-mPEG, followed by NA conjugation.

4.4.2.2 Characterisation by DLS

Figure 4.8 represents the size and zeta potential of the samples with different concentration of silane-PEG-NHS before and after functionalisation and conjugation. Functionalisation with NHS ester did not significantly affect the size (≈ 116-122 nm) or zeta potential (≈ -6 - -8 mV). However, conjugation with NA resulted in an observable increase in the size (≈

130 nm) for sample functionalised with 3% silane-PEG-NHS. This may be likely due to the large number of NA molecules on its surface, as before. In comparison, use of <1% silane-PEG-NHS in the silane-PEG reagent mixture lead to stable SNP-NA conjugates. The nature of the NA binding to SNP was evaluated using the biotin binding assay.

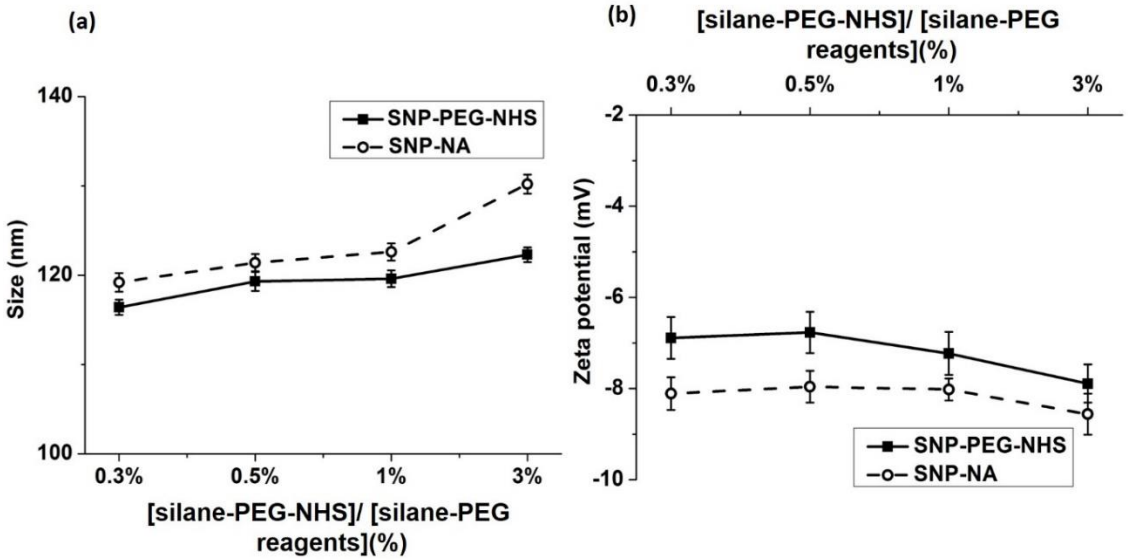

Figure 4.8: Colloidal properties, (a) size and (b) zeta potential, of SNP functionalised with 60 mM silane-PEG reagents, before (solid line) and after conjugation (dashed line) with NA, as measured by DLS. The fraction of silane-PEG-NHS in the silane-PEG reagent mixture was varied.

4.4.2.3. Characterisation by Biotin Binding

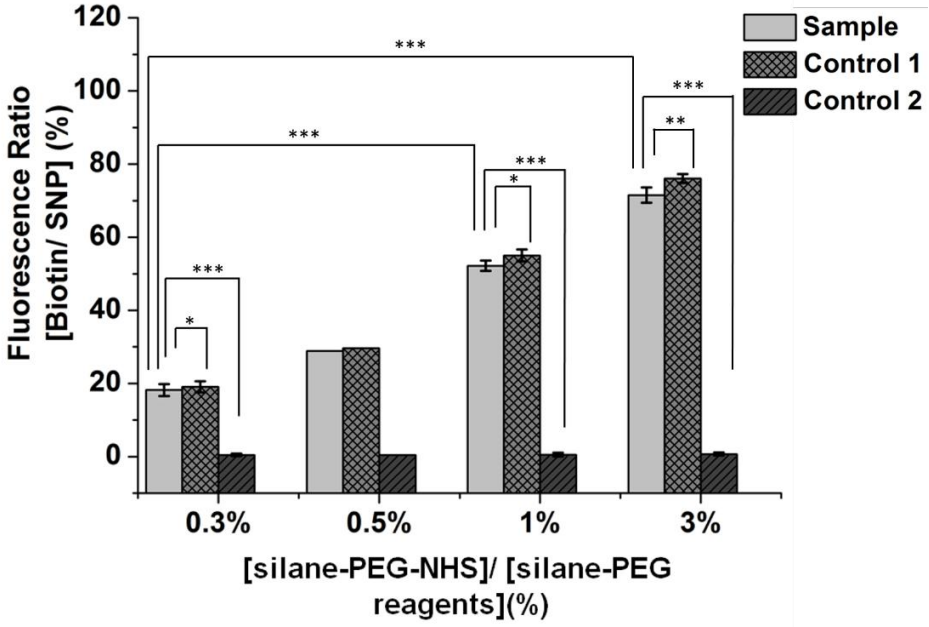

Figure 4.9 Biotin binding, as measured by a fluorescence-based assay, of SNP conjugated with NA. SNP was first functionalised with 60 mM silane-PEG reagents containing varying silane-PEG-content, and conjugated with 20 µM of NA (see text for conjugation details). In control 1, NHS was inactivated with ethanolamine to test for covalent nature of NA conjugation; NHS-functionalised SNP (without NA) treated with fluorescent biotin served was used in control 2 to test non-specific biotin binding and reliability of the assay. *, ** and *** indicates *P*-value < 0.01, < 0.001 and < 0.0001 respectively analysed using a two-way Students T-test.

Figure 4.9 demonstrates that SNP functionalised with 3% silane-PEG-NHS had a greater biotin binding efficiency (≈ 72 %) as compared to 1% silane-PEG-NHS sample, suggesting that increase in the number of NHS reactive group subsequently leads to higher number of NA molecules on the surface. However, a similar amount of biotin binding was observed in Controls 1, indicating that almost all the NA is non-covalently bound to the SNP-PEG-NHS. We confirmed that this is not arising due to non-specific biotin-binding by using Control 2 (lacking NA). The observed correlation between the percentage of silane-PEG-NHS used and the amount of non-covalently bound streptavidin suggests that the NHS groups on the surface are the major source of protein adsorption. As it will be seen later in this chapter, the SNP-PEG-NHS also resulted in severe non-specific labelling of cells, further confirming that unreacted NHS groups were of highly adsorptive in nature.

We tested various experimental parameters to eliminate this non-specific protein adsorption, but these attempts were unsuccessful. It is possible that silane-PEG-NHS reagents sourced from another manufacturer may be more effective, but we did not pursue this. Instead, we designed and tested a third covalent chemistry based on highly specific click-chemistry based reagents.

4.4.3 Click chemistry

4.4.3.1 Chemistry and Strategy

Azide-functionalised SNP was used to covalently immobilise alkyne modified NA in a single step reaction because of strong reactivity and specificity between azide and alkyne groups (Section 3.3.3). In the first step of this approach, a commercially available NHS ester functionalized dibenzocyclooctyne (DBCO-NHS ester) was used to introduce alkyne moiety(-ies) into NA. In the second step, the azide-functionalised SNP was reacted with the alkynated NA, yielding a stable SNP-NA conjugate (Figure 4.10).

The reaction was optimised based on the various experimental parameters, including the molar fraction of silane-PEG-azide (0 to 10%), molar ratio of DBCO-NHS ester to NA during alkynation, and controls to test for covalent nature of the bonding in SNP-NA conjugate. The alkyne modification of NA was tested using a control where the DBCO-NHS ester was first inactivated with ethanolamine (Control 2). The covalent conjugation between the azide and alkyne groups were tested by carrying out click-reactions with non-alkynated NA (Control 1). Any biotin-binding activity in these three controls would indicate adsorption of NA on the SNP-PEG-azide surface. All the conjugates (and controls) were also characterised by measuring their size and zeta potential by DLS.

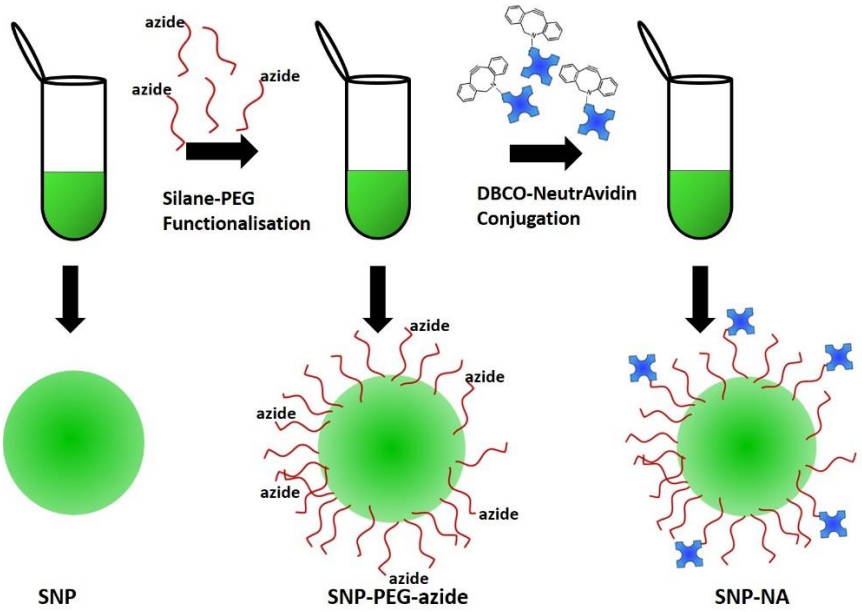

Figure 4.10 Schematic diagram of SNP functionalisation with a mixture of silane-PEG-azide and silane-mPEG, followed by click-chemistry based conjugation of NA using DBCO-NA.

4.4.3.2 Characterisation by DLS

The molar fraction of silane-PEG-azide in the silane-PEG reagent mixture was varied from 0.1 to 10% and the size and zeta potential of the samples were measured before and after functionalisation and conjugation (Figure 4.11). The sample with >=3% silane-PEG-azide showed increasing size after functionalisation. In comparison, click reactions carried out using SNP-PEG-azide functionalised with 0.1% and 1% silane-PEG-azide led to relatively stable SNP-NA conjugates, which were characterised further using the biotin-binding assay. However, this step required more optimisation since longer storage (>

1 week) of SNP-NA conjugates in PBS resulted in aggregation. The concentration of silane-PEG-azide and NA was tuned during conjugation to reduce aggregation occurring upon storage.

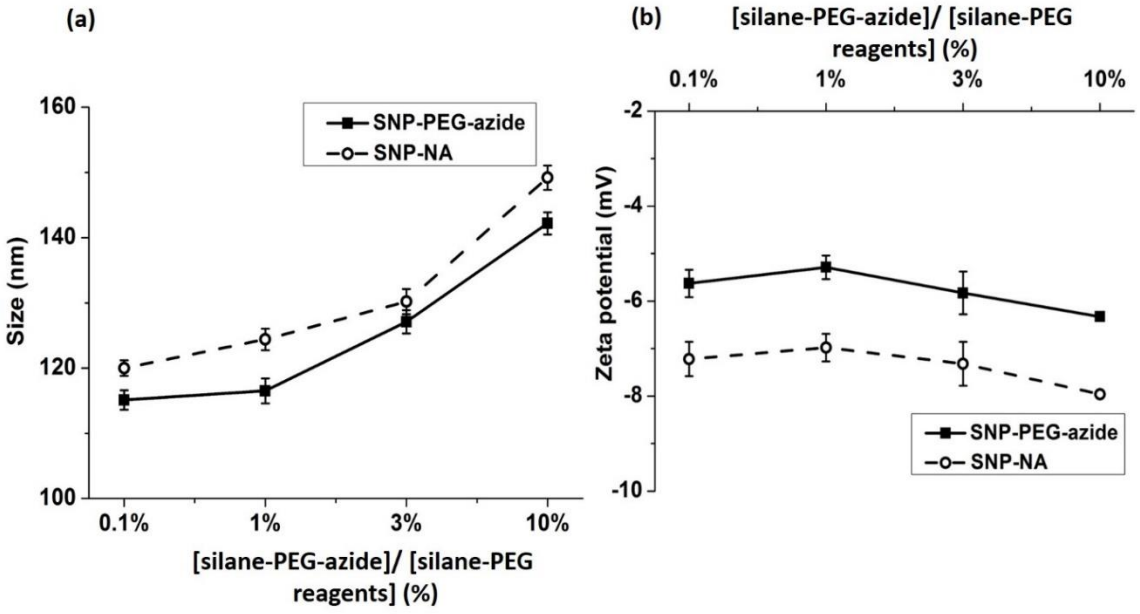

Figure 4.11: Colloidal properties, (a) size and (b) zeta potential, of SNP functionalised with 60mM silane-PEG reagents, before (solid line) and after conjugation (dashed line) with NA, as measured by DLS. The molar ratio between silane-PEG-azide and silane-mPEG was varied.

4.4.3.3 Characterisation by Biotin Binding

Figure 4.12 showed that SNP functionalised with 1% silane-PEG-azide had a greater biotin binding value (≈ 110%) as compared to 30 % for the 0.1% silane-PEG-azide sample, suggesting that 1% silane-PEG-azide SNP sample had a higher number of conjugated NA molecules. However, 1% silane-PEG-azide reagent was not used for further experiments due to the aggregation problem described earlier.

In addition to the high efficiency of conjugation, the click-chemistry based method also resulted in minimal non-specific biotin binding in the controls. For example, the values for Controls 1 and 2 were 1.6% and 3%, respectively. Very low biotin binding (3%) was also observed when SNP lacked azide functional groups.

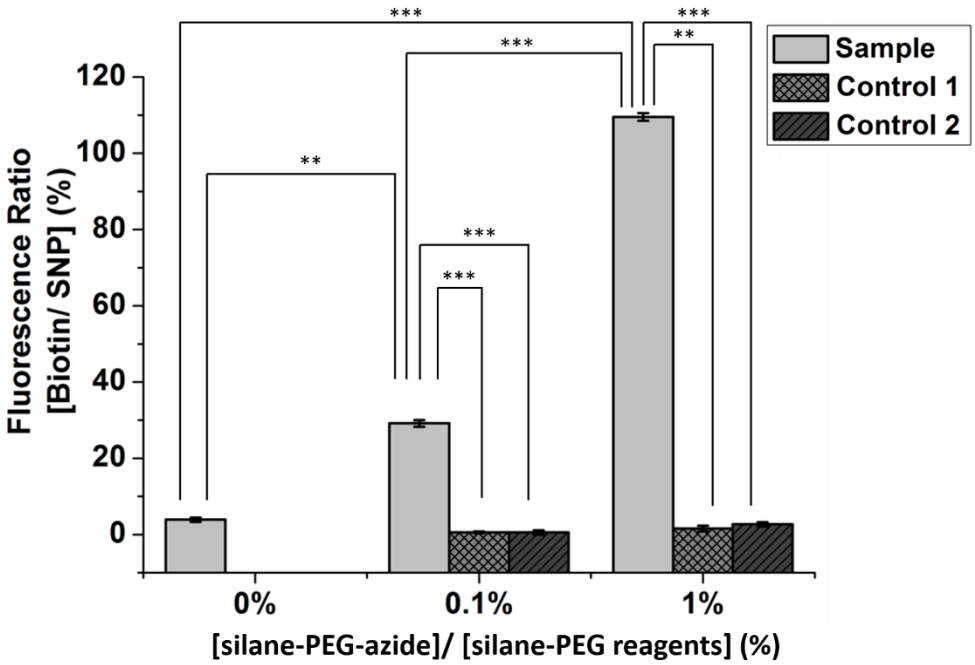

Figure 4.12: Biotin binding, as measured by a fluorescence-based assay, of SNP conjugated with NA. SNP was first functionalised with 60 mM silane-PEG reagents containing varying fractions of silane-PEG-azide, and conjugated with NA. In control 1, NA was used instead of DBCO-NA to test the specificity of the click reaction; and in control 2, DBCO-NHS was inactivated with ethanolamine before NA addition, to test for covalent nature of DBCO-NA reaction with azide-groups on SNP. ** and *** indicates *P*-value < 0.001 and < 0.0001 respectively analysed using a two-way Students T-test.

4.5 Application of fluorescent biofunctional SNP-NA conjugate

4.5.1 Labelling and imaging of μ-opioid receptors (MOR)

We tested if the developed SNP-NA conjugate from each of the conjugation chemistry can be used to label MOR in cells. The two-step labelling procedure is shown in Figure 4.13 (a). Briefly, the hemagglutinin-epitope tagged MOR was first targeted using a biotinylated antibody (Section 3.5). SNP-NA bound to the biotin tags on the antibody, thus indirectly labelling the MOR.

Figure 4.13 (c) shows an image of MORs labelled in fixed cells with SNP-NA conjugates developed using carbodiimide chemistry. The MOR labelling by these conjugates is poor and is not significantly different from the negative control (cells expressing MOR with FLAG-epitope tag, refer to 3.5). This result is comparable to the biotin binding presented in Figure 4.6. Together, these results indicate that either the carbodiimide based SNP-NA conjugation reaction is not efficient, or that this chemistry

renders the NA non-functional. We confirmed that the observed lack of labelling was not due to the poor functioning of the labelling procedure by using a fluorescently tagged streptavidin analogue (ExtrAvidin-FITC) as a positive control, as shown in Figure 4.13 (d-e).

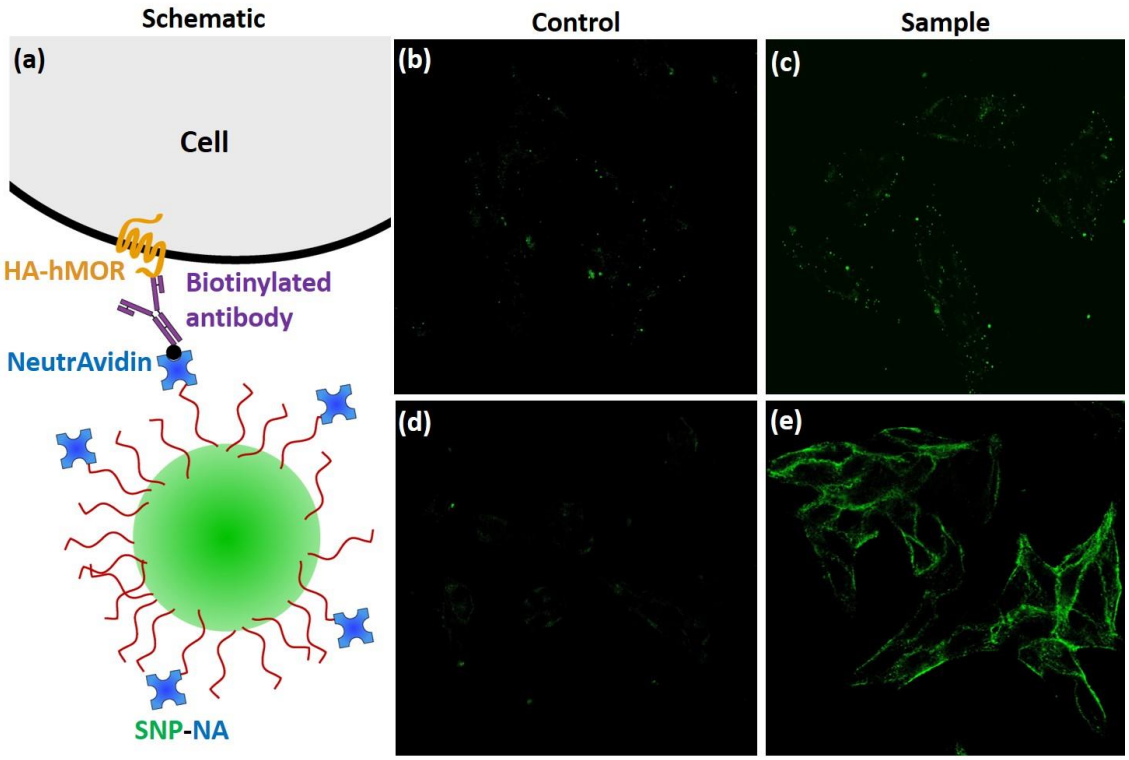

Figure 4.13 Labelling of HA-hMORs in fixed cells in two steps using SNP-NA conjugate, as schematised in (a), prepared using COOH functionalised SNP (b-c). (d-e) represents a positive control where FITC-conjugated Extravidin labelled the HA-hMORs, showing the expected labelling. Control was labelling of FLAG-mMORs. Image dimensions are 246 µm x 246 µm.

SNP-NA conjugates developed using NHS ester and click chemistry were used for labelling in both fixed and live cells. Comparison of specific and non-specific labelling in Figure 4.14 (a-d) shows that SNP-NA conjugates developed using NHS ester chemistry was prone to non-specific binding in both fixed and live cells. This, observation combined with the biotin binding data (Figure 4.9) further confirms that NHS groups on the SNP surface were highly adsorptive in nature, and it even bound to glass substrates (data not shown).

Figure 4.14 (e-h) show images of MORs labelled with SNP-NA conjugates developed using the click chemistry protocol, in fixed and live cells along with negative

controls. The MOR labelling by these conjugates was reproducible and highly reliable. This method resulted in the similar levels of the labelling of live and fixed cells. The labelling was observable over the entire cell membrane, where the MOR is expressed in basal conditions[9]. The non-specific binding was remarkably negligible. The dramatic reduction of the non-specific binding can be attributed to the high specificity and efficiency of the covalent click chemistry, as was also seen in the biotin-binding data (Figure 4.12).

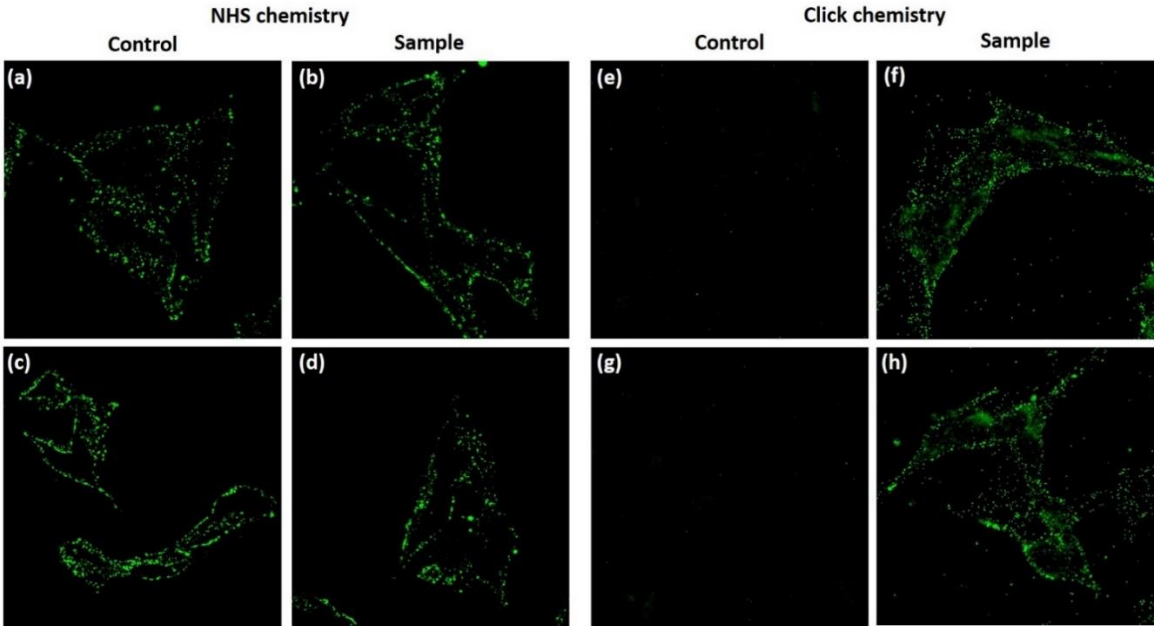

Figure 4.14 Labelling of HA-hMORs in (top row) fixed and (bottom row) live cells in two steps using SNP-NA prepared either using SNP-PEG-NHS (a-d) or SNP-PEG-azide (e-h). Control was labelling of FLAG-mMORs, which was not recognised by the antibody. Image dimensions are 130 µm x 130 µm (a-d) and 155 µm x 155 µm (e-h).

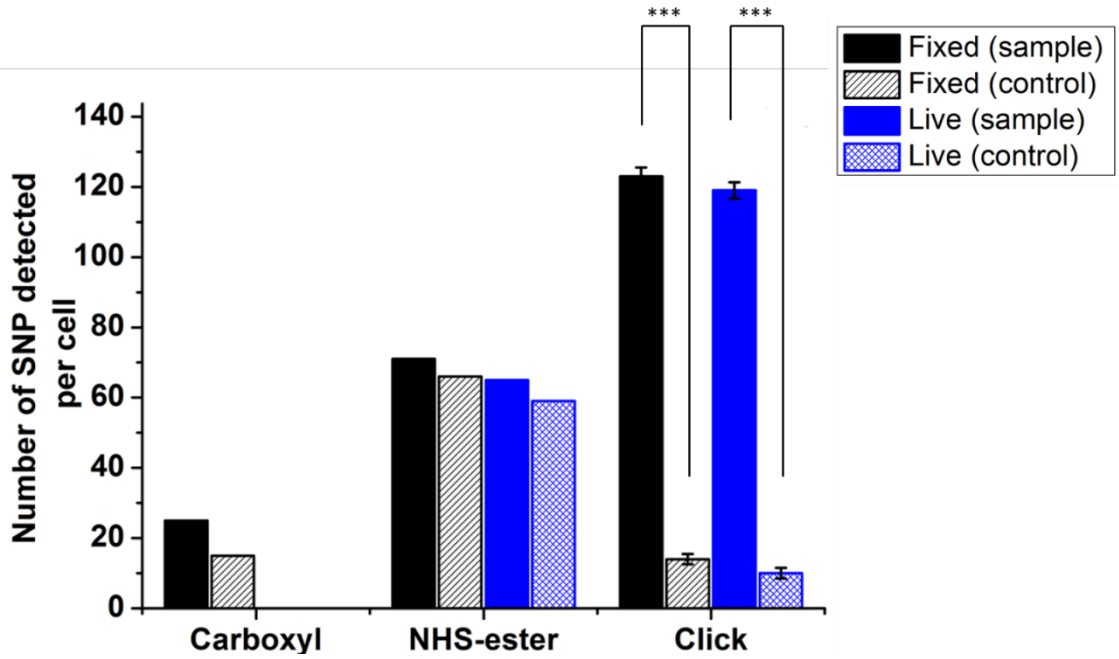

Figure 4.15 The number of SNP detected per cell in fixed and live cells in two steps using SNP-NA prepared either using SNP-PEG-carboxyl, SNP-PEG-NHS or SNP-PEG-azide. Control was labelling of FLAG-mMORs, which was not recognised by the antibody. *** indicates *P*-value < 0.0001 analysed using a two-way Students T-test.

4.6 Summary

Fluorescent silica nanoparticles (SNP) are a suitable model nanoparticle for testing and optimising conjugation reactions for other silica coated nanoparticles, including nanoruby. One of the biggest hurdles towards achieving a functional nanoparticle-protein conjugate is to develop a suitable method of functionalisation to covalently conjugate biomolecules on the SNP surface. Silane-based chemistry was found to be a suitable strategy to introduce either of the three different chemical groups (COOH; NHS-ester; azide) to the surface of SNP. These reactive groups used to covalently conjugate NA on the SNP, with varying success. Both the amide-based methods (COOH and NHS-ester) resulted in a low covalent conjugation efficiency exacerbated by considerable non-specific binding. In contrast, the click chemistry approach resulted in the efficient covalent conjugation and demonstrated minimal non-specific binding. At optimised reagent concentrations, the functionalised and conjugated nanoparticles also showed remarkable stability in water and physiological buffers. Moreover, the click chemistry method was robust and reliable, yielding conjugates suitable for fluorescent labelling of membrane receptors in live and fixed cells. This robust conjugation strategy was extended for

functionalising silica-coated ruby nanoparticles with NeutrAvidin, as described in the next chapter.

References

1. Mader, H., et al., *Fluorescent silica nanoparticles.* Annals of the New York Academy of Sciences, 2008. **1130**(1): p. 218-223.
2. Gerion, D., et al., *Synthesis and properties of biocompatible water-soluble silica-coated CdSe/ZnS semiconductor quantum dots.* The Journal of Physical Chemistry B, 2001. **105**(37): p. 8861-8871.
3. Lee, C.H., et al., *Synthesis and Characterization of Positive-Charge Functionalized Mesoporous Silica Nanoparticles for Oral Drug Delivery of an Anti-Inflammatory Drug.* Advanced Functional Materials, 2008. **18**(20): p. 3283-3292.
4. Akl, M., et al., *Preparation and characterization of silica nanoparticles by Wet mechanical attrition of white and yellow sand.* Journal of Nanomedicine & Nanotechnology, 2013. **4**: p. 2.
5. Meder, F., et al., *Protein adsorption on colloidal alumina particles functionalized with amino, carboxyl, sulfonate and phosphate groups.* Acta biomaterialia, 2012. **8**(3): p. 1221-1229.
6. Yang, Y.-C., et al., *Examination of dispersive properties of alumina treated with silane coupling agents, by using inverse gas chromatography.* Powder Technology, 2009. **191**(1): p. 117-121.
7. Laurent, S., et al., *Magnetic iron oxide nanoparticles: synthesis, stabilization, vectorization, physicochemical characterizations, and biological applications.* Chemical reviews, 2008. **108**(6): p. 2064-2110.
8. Moore, T.L., et al., *Nanoparticle colloidal stability in cell culture media and impact on cellular interactions.* Chemical Society Reviews, 2015. **44**(17): p. 6287-6305.
9. Galés, C., et al., *Real-time monitoring of receptor and G-protein interactions in living cells.* Nature methods, 2005. **2**(3): p. 177-184.

Chapter 5. Results on the functionalising photoluminescent Silica-coated Ruby Nanoparticles

The goal of this thesis is development of NeutrAvidin conjugated nanoruby particles, enabling labelling of μ-opioid receptors in live cells for the single molecular-sensitivity imaging. A robust and reliable method for conjugation of NeutrAvidin to model silica particles was developed in Chapter 4. In this chapter, the extension of the developed conjugation strategy to silica coated nanoruby (SiNR) is presented. This is followed by demonstrating the fluorescent labelling of receptors in live cells at the single particle sensitivity.

Contents

5.1 Characterisation of silica-coated ruby nanoparticles (SiNRs)

Silica-coated nanorubies were produced in house. Silica coating was used to overcome difficulties stemming from functionalising the as-produced nanoruby surface [manuscript in preparation]. SiNRs were thoroughly characterised in terms of their size, zeta potential and fluorescence spectra. The hydrodynamic diameter of SiNR was measured by DLS (section 3.1.1) to be 109 nm ± 2 nm. The zeta potential of SiNR was characterised by DLS to be -32 ± 1 mV (section 3.1.1) similar to that of the model silica nanoparticle (Section 4.2). The fluorescence spectra of nanoruby shown in Figure 5.1 confirmed the ruby-like photoluminescence characteristics.

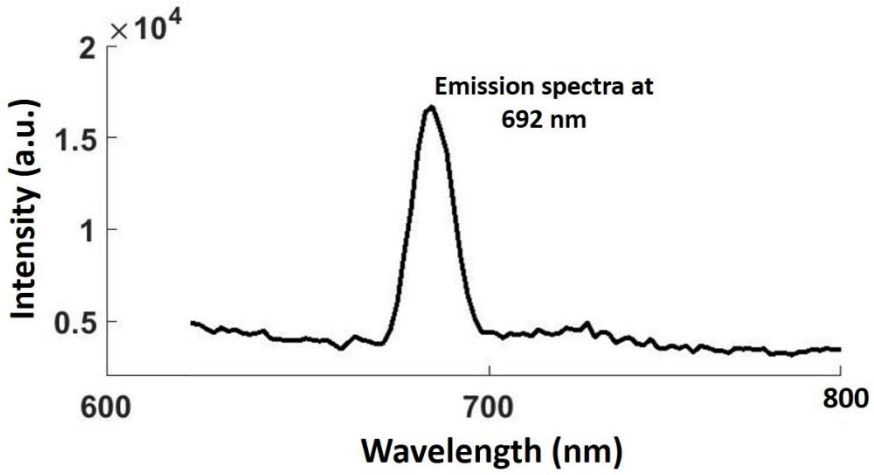

Figure 5.1 Emission spectra of SiNR sample under excitation of 532nm showing ruby like photoluminescence characteristics. The large spectral width of the peak (actual 4 nm) is due to the width of the spectral acquisition window.

5.2 Silane-based azide functionalisation of SiNR

SiNR was firstly functionalised using silane-PEG reagent mixture containing silane-mPEG and silane-PEG-azide, as described in Section 4.4.4.

5.2.1 Characterisation of azide functionalised SiNR

The size and zeta potential of the functionalised SiNR-PEG-azide were measured. Table 5.1 shows a slight increase in size when functionalised with silane-PEG-reagent mixture containing 1% silane-PEG-azide, as compared to 0.1%, concomitant with a slight decrease in zeta potential. This result is similar to that observed in azide-functionalised SNP (Figure 4.11), where a further increase in the percentage of silane-PEG-azide resulted in the severe aggregation of functionalised SNP.

5.3 Covalent conjugation of functionalised SiNR with NeutrAvidin

The click-chemistry reaction conditions optimised for SNP was implemented directly to conjugate SiNR-PEG-azide with alkynated NA, resulting in stable a SiNR-NA conjugate.

5.3.1 Characterisation of SiNR-NA conjugate

The SiNR-NA conjugates were characterised thoroughly for their size and zeta potential by DLS and biological activity of NA by biotin-binding assay.

5.3.1.1 Characterisation by DLS

Table 5.1 summarizes the size and zeta potential values of SiNR functionalised with silane-PEG-reagent mixture containing either 0.1% or 1% of silane-PEG-azide, and subsequently conjugated with NA. The increase in the number of azide groups (1% compared to 0.1%) caused an appreciable increase in the size after NA conjugation (126 nm compared to 119 nm). However, this increase did not appear to compromise the colloidal stability of the conjugate even in PBS, as confirmed by visual inspection.

Samples	[silane-PEG-azide]/ [silane-PEG reagents] (%)	Size (nm)	Zeta (mV) in water
SiNR	-	109	-32
SiNR-PEG-azide	1	118	-28
	0.1	112	-31
SiNR-NA	1	126	-26
	0.1	119	-29

Table 5.1 Colloidal properties (size and zeta potential) of unfunctionalized SiNR, azide-functionalised SiNR and NeutrAvidin-conjugated SiNR, as measured by DLS. Two molar fractions of silane-PEG-azide were tested, but the total concentration of the silane-PEG reagent mixture was maintained at 60 mM.

5.3.1.2 Characterisation by biotin binding

Figure 5.2 represents the biotin binding data for SiNR-NA conjugate functionalised with 1% silane-PEG-azide. Minimal biotin binding was observed for the control prepared

with non-alkynated NA. The large difference (41% compared to 2%) between the biotin binding in the sample and control indicated highly specific and covalent conjugation, similar to that observed in SNP-NA conjugation experiments.

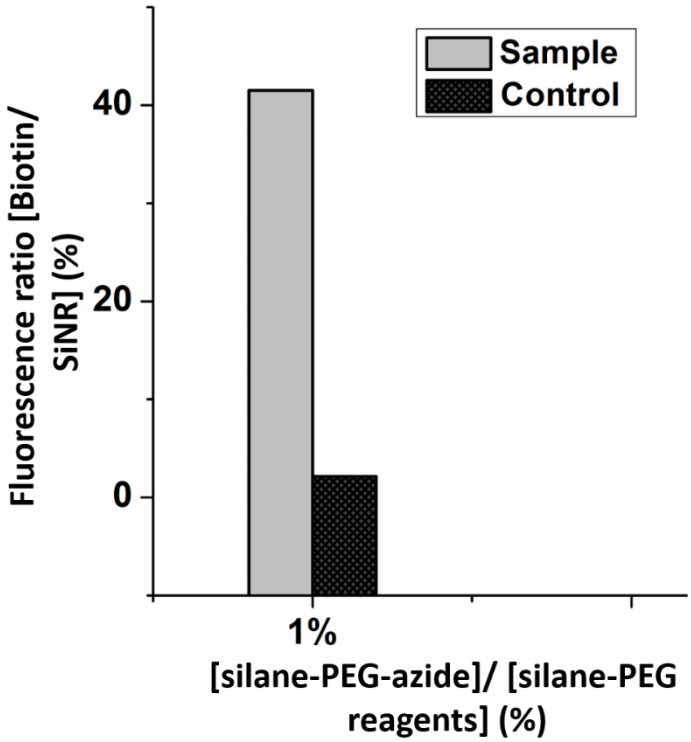

Figure 5.2 Biotin binding, as measured by a fluorescence based assay, for SiNR functionalised with 60 mM silane-PEG reagents, containing 1% silane-PEG-azide, followed by conjugation with NA. Control corresponds to reaction carried out using NA instead of DBCO-NA to test the specificity of click chemistry.

5.4 Application of fluorescent biofunctional SiNR-NA conjugate

Biotin-functionalised silica-coated nanoruby was previously used to label μ-opioid receptors (MOR) using a three-step streptavidin-sandwich labelling method described in Section 1.1 (Motivation of research). While the method was successful in labelling MOR in fixed cells, the efficiency of live labelling was poor. It was hypothesized that reduction of the labelling procedure to two steps by directly conjugating streptavidin (or NeutrAvidin) onto silica coated nanoruby would improve the labelling in both live and fixed cells. Here we report on testing of this hypothesis using SiNR-NA developed by click-chemistry.

5.4.1 Labelling and imaging of μ-opioid receptors

The procedure of two step labelling of MOR using SiNR-NA is schematised in Figure 5.3 (a). Briefly, hemagglutinin-epitope tagged MOR expressed on the surface of AtT20 cells was first targeted using a biotinylated antibody (Section 3.5). SiNR-NA then bound to the biotin tags on the antibody, thus indirectly labelling the MOR. Figure 5.3(e) and (i) shows images of MORs labelled in fixed and live cells, which show similar levels of labelling. Comparison with negative controls indicates that the labelling is highly specific with minimal background binding. These results further confirm the biotin binding data presented in Figure 5.2 that SiNR has been successfully and covalently conjugated to NA. This result also suggests that the discrepancy observed between live and fixed cell labelling using three-step streptavidin-sandwich method arises due to the multiple steps in the labelling procedure. We show that such discrepancies can be minimised by directly conjugation NeutrAvidin to the nanoruby.

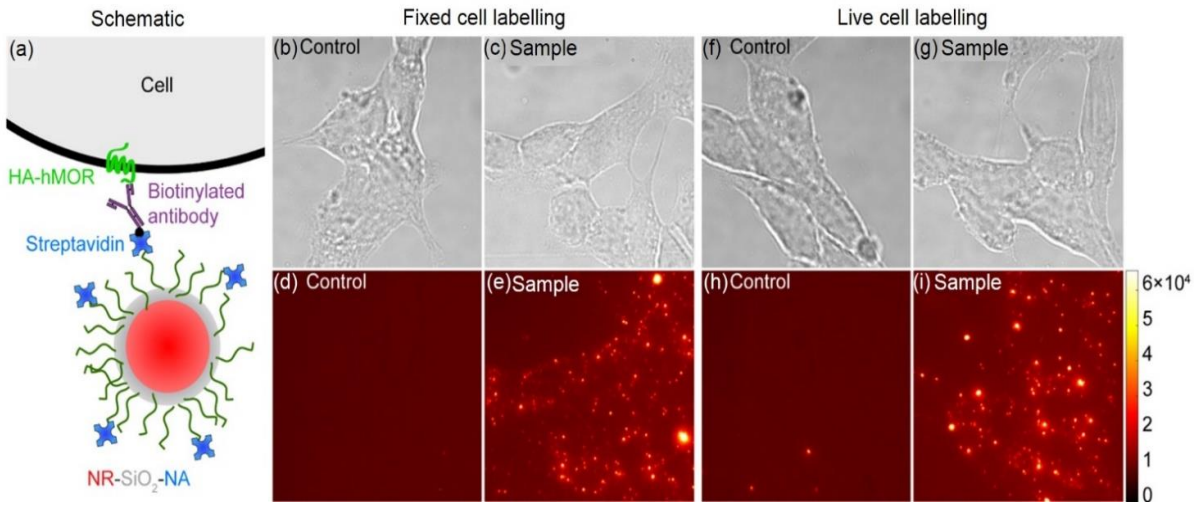

Figure 5.3 Cell labelling of HA-hMOR in (b-e) fixed cells (f-i) and live cells in two steps using SiNR-NA conjugate, as schematised in (a), prepared using SiNR-PEG-azide. Control was labelling of FLAG-mMORs, which was not recognised by the biotinylated antibody. Bright field images to visualise the cell morphology are shown in greyscale (top row). The nanoruby photoluminescence image is shown in false colour (bottom row), and the corresponding color bar is shown on bottom right. Image dimensions are 130 μm x 130 μm each.

5.5 Discussion and Summary

Fostering widespread applications of silica-coated ruby nanoparticles in molecular imaging requires development of facile and reproducible surface functionalisation procedures. Click chemistry was found to be a very efficient technique to functionalise silica-coated ruby nanoparticles with biomolecules, such as NeutrAvidin. It resulted in reliable covalent SiNR-NA conjugate, which demonstrated remarkably small non-specific binding with high efficiency receptor labelling. We successfully demonstrated the applicability of these conjugates towards labelling of MORs in both fixed and live cells, which was previously not possible using the three-step labelling procedure. This novel strategy is believed to be promising for robust and reproducible functionalisation of a variety of nanoparticles and biomolecules.

Chapter 6. Summary and Future Perspective

6.1 Summary

Fluorescence microscopy is a powerful tool for visualising tissues, cells and biomolecules, and has been instrumental in increasing our understanding of complex biological interactions. The integration of fluorescence microscopy with probes based on photoluminescent (PL) nanoparticles (NPs) is rapidly emerging due to its several advantages over conventional molecular probes. This trend shows that PL NPs that feature high photostability and allow ultrasensitive detection and imaging are in high demand. Silica-coated nanoruby (SiNR) have previously shown to exhibit remarkable photostability and long emission lifetimes, meeting these requirements. However, the application of SiNR in Life Sciences has been limited due to difficulties in surface functionalisation and conjugation of biomolecules.

In this work, silane-based chemistry was found to be a stable and reproducible method to functionalise the silica surfaces. The process improved the colloidal stability of the nanoparticles, and prepared their surface for subsequent conjugation by grafting reactive moieties such as carboxyl, NHS ester and azide groups. Using the three different functional groups, three different covalent conjugation strategies were tested on a model silica nanoparticles. Among them, the click chemistry was found to be the most efficient, reliable and reproducible strategy for conjugating the nanoparticles with NeutrAvidin (a streptavidin analog). We extending the click chemistry strategy to conjugate silica-coated nanoruby with NeutrAvidin. Using this nanoruby conjugate, we demonstrated the specific labelling and single-particle sensitive imaging of μ-opioid receptors in live and fixed cells.

In summary, our study enabled efficient functionalisation and application of silica-coated nanoruby towards highly specific labelling and sensitive imaging of biologically significant molecules such as μ-opioid receptors in living tissues.

6.2 Future scope

The developed PL NP-based probe has far-reaching prospects. Firstly, the NeutrAvidin conjugated nanoruby can be used to elucidate intracellular dynamics of opioid drug-receptor interactions by live imaging. Here, the unlimited photostability of nanoruby can be used visualise receptor processes occurring at the timescales of milliseconds to hours, such as membrane diffusion, rapid endocytosis, intracellular transport and slow recycling. The long photoluminescence lifetime of nanoruby, in combination with time-

gated can enable sensitive visualisation of single drug-receptor complexes even in brain tissue slices by suppressing tissue fluorescence. The entire process of ligand-receptor interaction, beginning from the binding, to receptor activation, to internalisation, trafficking and recycling/degradation can be investigated, not only for μ-opioid receptors, but for any transmembrane receptor or extracellular protein in general. The outcomes of this work are, therefore, believed to be of immediate interest to the entire Life Sciences and Nanotechnology community.

Supporting Information

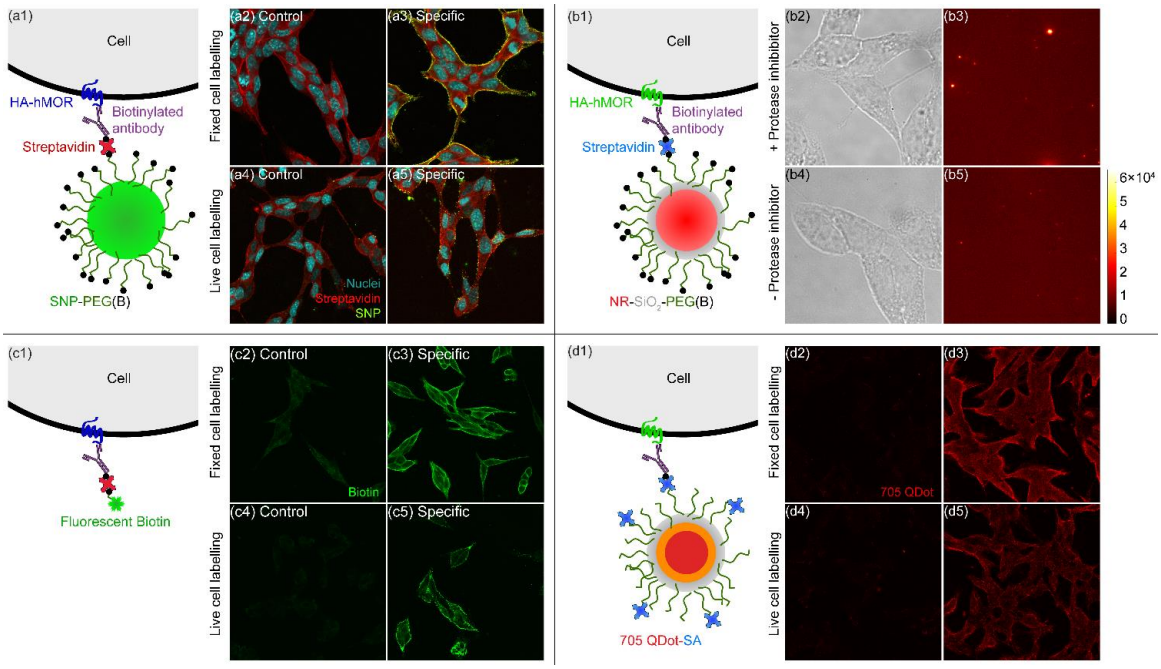

Figure S1. (a1-a5) Labelling of μ-opioid receptors in fixed and live cells using biotinylated fluorescent silica nanoparticles (SNP-PEG(B)) in three steps. Labelling is much less efficient in live cells when compared to fixed. (a1) is a schematic representation of the three-step labelling procedure. The colour legend is shown in the bottom right corner of (a4). The yellow color is due to co-localisation of streptavidin and SNP. Image dimensions are 155 μm × 155 μm.

(b1-b5) Labelling of μ-opioid receptors in live cells using NR-SiO_2-PEG(B) in three steps, in the (b2, b3) presence or (b4, b5) absence of a protease inhibitor cocktail (P8340, Sigma Aldrich). The protease inhibitor does not improve receptor labelling in live cells. (b1) is a schematic representation of the three-step labelling procedure.. (b2, b4) Bright field images to visualize the cell morphology are shown in greyscale, whereas (b3, b5) nanoruby time-gated photoluminescence images are shown in false colour, based on a colour look-up-bar shown at the bottom-right corner. Image dimensions are 91 μm × 91 μm.

(c1-c5) Labelling of μ-opioid receptors in fixed and live cells using fluorescent biotin (PromoFluor-555P, biotin, Jomar Life Research), in three steps. The extent of labelling is similar in both fixed and live cells. (c1) is a schematic representation of the three-step labelling procedure. The colour legend is shown in the bottom right corner of (c2). Image dimensions are 246 μm × 246 μm.

(d1-d5) Labelling of μ-opioid receptors using streptavidin-coated 705 QDot in fixed and live cells, in two steps. Labelling in live cells is robust, albeit being slightly lower than in fixed cells. (d1) is a schematic representation of the two-step labelling procedure. The colour legend is shown in the bottom right corner of (d2). Image dimensions are 246 μm × 246 μm.

Appendix

“This project did not need an ethics approval, only a biosafety approval. The approval includes the user Varun Sreenivasan (my supervisor), who handled the cells.” The following is the biosafety approval letter.

Approval for Exempt Dealing “Regulation of receptors and ion channels in vitro" (5201500367)

Bio Safety

Fri 08/05/2015 14:34

To:Mark Connor <mark.connor@mq.edu.au>;

Importance: High

Re: Exempt Dealing, “Regulation of receptors and ion channels in vitro" (5201500367)

Thank you for your response to concerns raised by the Institutional Biosafety Committee (IBC) regarding the above application. The Chair has reviewed your response and approval of the above Exempt Dealing has been granted, effective 4 May 2015.

Approval has been granted subject to your compliance with the Office of the Gene Technology Regulator’s standard conditions for exempt work listed below:

1. The project must be conducted in accordance with the OGTR Guidance Notes for the Containment of Exempt Dealings (http://www.ogtr.gov.au/internet/ogtr/publishing.nsf/Content/ExemptDealGuideSept11_2-htm

2. The Guidance Notes are only applicable to exempt dealings conducted under the *Gene Technology Act 2000*. They do not provide guidance for laboratory safety, good laboratory practice or work health and safety issues. For these purposes, refer to AS/NZS 2243.3:2010.

3. You must inform the Institutional Biosafety Committee if you complete or abandon the exempt dealings with GMOs.

Please note the following standard requirements of approval:

1. Approval will be for a period of 5 years *subject to the provision of annual reports* (http://www.research.mq.edu.au /current_research_staff gene_technology_and_biosafety/submitting_a_new_application). If, at the end of this period the project has been completed, abandoned, discontinued or not commenced for any reason, you are required to submit a Final Report. If you complete the work earlier than you had planned you must submit a Final Report as soon as the work is completed. Please contact the Committee Secretary at biosafety@mq.edu.auin order to obtain a report.

A Progress/Final Report for this project will be due on: 04 May 2016.

2. If you will be applying for or have applied for internal or external funding for the above project it is your responsibility to provide the Macquarie University’s Research Grants Management Assistant with a copy of this email as soon as possible. Internal and External funding agencies will not be informed that you have final approval for your project and funds will not be released until the Research Grants Management Assistant has received a copy of this email.

If you need to provide a hard copy letter of Final Approval to an external organisation as evidence that you have Final Approval, please do not hesitate to contact the Committee Secretary at biosafety@mq.edu.au or by phone 9850 4063.

Please retain a copy of this email as this is your formal notification of final Biosafety approval.

Yours Sincerely

Biosafety Secretariat
Research Office
Level 3, Research Hub, Building C5C East
Macquarie University
NSW 2109 Australia

T: +61 2 9850 4063
F: +61 2 9850 4465

http://www.mq.edu.au/research

--
Macquarie University Biosafety Secretariat
Research Office
Level 3, Research HUB, Building C5C
Macquarie University
NSW 2109

Ph: +61 2 9850 6845

Email: biosafety@mq.edu.au